

Daniel Kjellevold Steinsland

Analysis of traffic with two lanes using numerical and analytical methods

Master's thesis in MTFYMA
Supervisor: Helge Holden
July 2022

Daniel Kjellevold Steinsland

Analysis of traffic with two lanes using numerical and analytical methods

Master's thesis in MTFYMA
Supervisor: Helge Holden
July 2022

Norwegian University of Science and Technology
Faculty of Information Technology and Electrical Engineering
Department of Mathematical Sciences



Abstract

In the following, we analyse traffic flow in a system with two lanes. We study a Lighthill-Whitham-Richards (LWR) type model with the added complexity of two lanes where vehicles are assumed to always switch to the neighbouring lane if vehicles in that lane are moving faster. The resulting model is then a weakly coupled system of hyperbolic conservation laws.

We start by presenting a numerical scheme for weakly coupled hyperbolic conservation laws. This scheme is based on the use of operator splitting. Combining finite volume methods with an explicit Euler scheme. We will provide proof of the convergence of this scheme.

After presenting this numerical method, we show results from some simulations of the traffic model. We comment on these results and suggest what might be the asymptotic behaviour in time of the model. In particular, we will look at if the velocities in the two lanes become equal asymptotically.

We will finish with a closer look at the analytical properties of the model for traffic flow. This will consist of looking at special cases and what asymptotic behaviour in time these cases will show. We will especially look at which cases give a difference in velocity going to zero after a long time.

Samandrag

Vi kjem her til å sjå nærare på trafikkflyt i system der det er to felt med køyretøy som køyrer i samme retning. Modellen me skal sjå på er ein Lighthill-Whitham-Richards type modell i kvart felt. Saman med ei antaking om at køyretøy alltid vil skifte til det feltet der køyretøya har høgast hastighet. Modellen vi då ender opp med er eit system av svakt kopla hyperbolske konserveringslover.

For å analysere slik trafikk starter vi med å etablere metoden vi skal benytte for simuleringar. Vi kjem då til å benytte ein klasse numeriske skjema som blir basert på operator splitting. Der vil vi då kombinere endeleg volum metodar og eit eksplisitt Euler skjema, som vi også gir eit bevis for at konvergerer.

Etter at vi har presentert metoden vi skal nytte for simuleringane skal vi gjengi nokre resultat frå simuleringane. Vi kjem då også til å peike ut nokre trekk som går igjen, og nytte dette til å anmode kva eigenskapar vi gjerne vil vise analytisk at held for modellen. I dette kjem vi særleg til å sjå på om utviklinga i tid av trafikkflyten vil føre til like hastigheter i dei to felta asymptotisk.

Vi avslutter så med ein seksjon der vi forsøker å analytisk vise at dei eigenskapane simuleringane anmoder virkelig stemmer. Her kjem vi særleg til å sjå på nokon enklare eksempel der vi kan vise direkte om hastighetane i dei to felta blir like eller ikkje.

Preface

This thesis was written in the spring of 2022 and is the conclusion of a five-year study program in applied physics and mathematics. All work I present in this thesis was done over this same semester. However, a great deal of groundwork was laid in my project thesis, which I wrote in the fall of 2021.

I want to thank my supervisor, Helge Holden, for the time, guidance and support he has given me in writing this thesis. For an exciting problem to work on and great help every time I have asked for it.

I would also like to thank my wonderful family and friends for their support. In particular, I am thankful for my beloved fiance. Her constant love and support have been a great motivation for days when inspiration has been hard to find.

Contents

1	Introduction	1
2	Prerequisites, notation and definitions	4
2.1	Definitions and notation	4
2.2	Compactness theorems and inequalities	4
2.3	Entropy solutions	6
2.4	Operator splitting	7
2.5	Finite volume schemes	7
3	Results for numerical schemes	9
3.1	Convergence results	10
4	Simulations on multilane traffic flow	18
4.1	The Engquist-Osher scheme	19
4.2	Simulation results	21
4.2.1	General behaviour with periodic boundary conditions	21
4.2.2	Difference in velocity across lanes	23
4.2.3	Riemann problem simulations	26
4.2.4	Model interpretation	29
5	Analytical results regarding multilane traffic flow	31
5.1	General properties of the two lane system	31
5.2	Smooth case	32
5.3	Operator splitting	34
5.4	Effect from the source step	35
5.5	Equal velocity function in both lanes	36
5.6	A class of counterexamples	36
6	Conclusion and further work	39
A	Scaling the traffic equation	40

1 Introduction

Well the night's busting open
These two lanes will take us anywhere.

- Bruce Springsteen,
Thunder Road(1975)

One of the major challenges in infrastructure is traffic congestion. Often we look to solve this problem by building bigger and better roads. In particular, roads can be constructed to have more lanes going in the same direction. Multiple lanes provide room for more vehicles to drive down the road and cause a smoother traffic flow. However, multilane roads are also expensive to build and maintain, while also taking up much of the available space.

Therefore, great care must be placed in the planning of such projects. Some of the most important tools in such planning phases are the various models of traffic flow. These models are important tools in measuring how great the improvement in the flow of vehicles will be. Thus it is important to have models which are well understood and easily used. There are then two main concepts for modelling traffic flow. The first is to model individual vehicles, where the behaviour of each vehicle is decided from the current traffic picture. This approach is studied well in [1],[6], [23] among many sources, and we will not focus on this approach here.

The second type of traffic modelling is what we refer to as "traffic hydrodynamics", where we assume that the traffic is so dense that we may treat it as we would a fluid. This is the approach we will study today, in particular, we will study a Lithghill-Whitham-Richards (LWR) model. This approach was introduced in [17], [20] and has among others been studied in [7], [15]. We note also that given only a single lane, the "traffic hydrodynamics" approach can be obtained as a continuum limit of the individual vehicle approach [13], [14], [23].

Here we will study a model for multilane traffic flow first introduced in [15]. Before we give a short derivation of the model, we introduce some notation. In the following, $u_i(x, t)$ is the density of traffic in lane i , at time t , and position x along the road. The function $v_i(u_i)$ is the velocity function of lane i , and models the velocity vehicles will drive in at certain densities of traffic. We will require the velocity function to be differentiable and strictly decreasing, with some maximum value at $v_i(0) < \infty$ which is the speed limit (we think of $v_i(0)$ as the speed a single vehicle would hold if it is alone on the road).

We derive the model we will study from two assumptions. The first assumption is that if we ignore vehicles switching lanes, the flow of traffic behaves entirely like normal traffic flow. Following an LWR model, which would, for a single lane give the behaviour,

$$\partial_t u_i + \partial_x(u_i v_i(u_i)) = 0. \quad (1.1)$$

The second assumption is that the rate at which vehicles switch lanes is proportional to the difference in velocity between the two lanes, and the density of vehicles in the lane vehicles are leaving. The combination of these assumptions gives us the model

$$\begin{aligned} \partial_t u_1 + \partial_x(u_1 v_1(u_1)) &= -S(u_1, u_2), \\ \partial_t u_2 + \partial_x(u_2 v_2(u_2)) &= S(u_1, u_2). \end{aligned} \quad (1.2)$$

The source term here is defined as

$$S(u) = K(v_2(u_2) - v_1(u_1)) \begin{cases} u_2, & v_2(u_2) \leq v_1(u_1), \\ u_1, & v_2(u_2) > v_1(u_1), \end{cases} \quad (1.3)$$

and is used to model vehicles switching lanes. The constant K is used to model the rate at which vehicles are expected to switch lanes. We will assume K to be equal to one for the entire thesis, as we can rescale (1.2) such that K is equal to one, as shown in Appendix A. An important note is that given initial conditions contained entirely in $[0, 1]$, the solution will remain in $[0, 1]$ indefinitely, as shown in Lemma 2.4 of [15]. We will then study (1.2) both through numerical simulations and some analytical methods. To develop the tools needed for this, we first remark that the (1.2) is a system of weakly coupled hyperbolic conservation laws.

Weakly coupled systems of hyperbolic conservation laws are equations of the general form

$$\partial_t u_i + \partial_x f_i(u_i) = g_i(u), \quad u_i(x, 0) = u_{i,0}(x), \quad (1.4)$$

where f_i is a C^1 -function, $i = 1, \dots, d$ is an index and $g : \mathbb{R}^d \rightarrow \mathbb{R}$ is a Lipschitz continuous function. Such systems can typically come up in models where there is some conserved quantities, u_i , which is also affected by some external source of change. Then f_i models the change of the conserved quantity without the external effect. Meanwhile, g_i is used to model the external influence on u_i . Some examples of such applications are seen in [2], [12], [15]. This is a well studied class of equations, and requirements for existence and uniqueness of a solution are known. Referring to [12] and [18], we see that under the conditions that

$$g_i, f_i \in \text{Lip}_{loc}(\mathbb{R}^d; \mathbb{R}), \quad g_i(0) = f_i(0) = 0, \quad \forall i \in \{1, \dots, d\}, \quad (1.5)$$

then there exists a unique entropy solution to (1.4), given bounded initial conditions. Which can also be applied to (1.2), in order to prove existence and uniqueness.

In the case where $g_i = 0$, we see that equation i becomes a standard scalar conservation law. For such equations there is a rich literature we can pull from. Some examples can be seen in [3],[11],[16]. This fact will be one of the main motivations behind our choice of method, namely a operator splitting scheme, which will allow to use this literature.

For (1.4), it seems a natural choice to utilize a scheme based on splitting the operators as

$$\partial_t u_i + \partial_x f_i(u_i) = 0, \quad i = 1, \dots, d, \quad (1.6a)$$

$$\partial_t u = G(u). \quad (1.6b)$$

Where $u = (u_1, \dots, u_d)$, and $G(u) = (g_1(u), \dots, g_d(u))$. Such a splitting scheme is discussed in chapter 5 of [11]. Though in the following we will be focused specifically on a fully discretized scheme. This means using first order monotone, conservative, and consistent finite volume schemes in order to solve (1.6a) numerically, and using a simple forward Euler to solve (1.6b) numerically. We will provide a full proof of convergence for this method in Section 3.

This is then the type of scheme we will apply for the numerical simulations of (1.2). We will then use an Engquist-Osher scheme for the flux step, as this is known to conserve shocks well. Furthermore, for convex and concave flux functions, Engquist-Osher runs quite quickly. Therefore, all our simulations will be run with concave flux functions, which are obtained by using concave velocity functions. We will then proceed to do a detailed study of various simulations of (1.2). Utilizing various initial conditions, and models for velocity in the two lanes. We will then use these simulations to look at the asymptotic behaviour of solutions for (1.2). In particular, we will study the difference in velocity across the two lanes, through looking at the velocity difference functional, defined as

$$\mathcal{F}(u(\cdot, t)) = \int |v_2(u_2) - v_1(u_1)| dx. \quad (1.7)$$

In practical applications the asymptotic value of \mathcal{F} can tell us to what degree both lanes will be properly utilized. If we have traffic in two lanes where one lane is moving along much faster than the other, then the slow lane might not be too much with smoothing out the flow of traffic. The results from these simulations can be found in Section 4.

After an in-depth analysis of several simulations of (1.2), we will move on to looking at (1.2) from a more analytical point of view. In particular, we will establish some general theorems about the asymptotic behaviour of (1.2), and look at some special cases where we can place some bounds on the asymptotic value of \mathcal{F} . This more analytical approach is shown in Section 5.

2 Prerequisites, notation and definitions

In this section we introduce some important theorems, and concepts. These are well known from literature, so proofs will not be given here, instead references will be given.

2.1 Definitions and notation

For partial derivatives we will use the notation

$$\frac{\partial f}{\partial x_i}(x) = \partial_{x_i} f(x) = f_{x_i}(x).$$

We will for the most part prefer using the second of these as the subscript notation can be confusing when combined with a lot of indices.

We define a modulus of continuity to be a non-decreasing continuous function $\nu : [0, \infty) \rightarrow [0, \infty)$, such that $\nu(0) = 0$.

For Lipschitz continuous functions, we have the notation

$$\|f\|_{Lip} = \inf_{x \neq y} \frac{|f(x) - f(y)|}{|x - y|}.$$

For finding the greatest/least of two elements we will use the notation

$$u \vee v := \max\{u, v\}, \quad u \wedge v := \min\{u, v\}.$$

We will make use of the Heaviside function and the sign function, which we will denote

$$H_a(x) = \begin{cases} 0, & x \leq a, \\ 1, & x > a, \end{cases}$$

and

$$\text{sgn}(x) = \begin{cases} 1, & x > 0, \\ 0, & x = 0, \\ -1, & x < 0. \end{cases}$$

For the positive or negative parts of a function we use the notation

$$f(x)^+ = \frac{|f(x)| + f(x)}{2}, \quad f(x)^- = \frac{|f(x)| - f(x)}{2}.$$

Finally, we will also make use of the Iverson bracket notation for true and false statements, and sometimes as an indicator function,

$$[\text{Statement}(u)] = \begin{cases} 1, & \text{Statement}(u) \text{ is true,} \\ 0, & \text{Statement}(u) \text{ is false.} \end{cases} \quad (2.1)$$

2.2 Compactness theorems and inequalities

We will need to make use of some compactness results for convergence. We start out by stating the classic Kolmogorov's compactness theorem, as found in [9]

Theorem 2.1. *Let \mathcal{F} be a subset of $L^p(\mathbb{R}^n)$, $p \in [1, \infty)$. Then \mathcal{F} is relatively compact in $L^p(\mathbb{R}^n)$ if and only if the following conditions are satisfied:*

(i) for every $\varepsilon > 0$, there is some R so that for every $u \in \mathcal{F}$,

$$\int_{|x|>R} |u|^p < \varepsilon^p,$$

(ii) for every ε there is some $\rho > 0$ so that for every $u \in \mathcal{F}$, and every $y \in \mathbb{R}^n$ with $|y| < \rho$,

$$\int_{\mathbb{R}^n} |u(x+y) - u(x)|^p dx < \varepsilon^p.$$

For the analysis of PDE's this is the classic compactness theorem. For our studies, we will however prefer to use this next version. Which can be found in appendix A in [16].

Theorem 2.2. Let $u_\mu : \mathbb{R}^n \times [0, \infty) \rightarrow \mathbb{R}$ be a family of functions such that for each positive T ,

$$|u_\eta(x, t)| \leq C_T, \quad (x, t) \in \mathbb{R}^n \times [0, T],$$

for a constant C_T independent of η . Assume also that for all compact $B \subset \mathbb{R}^n$ and $t \in [0, T]$,

$$\sup_{|\xi| \leq |\rho|} \int_B |u_\eta(x + \xi, t) - u_\eta(x, t)| dx \leq \nu_{B,T}(|\rho|),$$

for a modulus of continuity $\nu_{B,T}$. Furthermore, assume that for s , and t in $[0, T]$,

$$\int_B |u_\eta(x, t) - u_\eta(x, s)| dx \leq \omega_{B,T}(|t - s|) \text{ as } \eta \rightarrow 0,$$

for some modulus of continuity $\omega_{B,T}$. Then there exists a sequence $\eta_j \rightarrow 0$ such that for each $t \in [0, T]$ the sequence $\{u_{\eta_j}\}$ converges to a function $u(t)$ in $L^1_{loc}(\mathbb{R}^n)$. The convergence is then in $C([0, T]; L^1_{loc}(\mathbb{R}^n))$.

Note that if we have a uniform bound on the spatial total variation on u_η , then the second of the requirements above will be satisfied.

We finish this section with the following useful inequality. We state a version of the discrete Gronwall inequality, where we refer to Theorem 2.1.2 of [19] and Exercise 2.17 from [10].

Lemma 2.3. Let k_n , and ϕ_n be sequences such that $k_n \geq 0$, and that ϕ_n satisfies the inequalities

$$\begin{aligned} \phi_0 &\leq g_0, \\ \phi_n &\leq g_0 + \sum_{m=0}^{n-1} k_m \phi_m, \quad n \in \mathbb{N}, \end{aligned}$$

then we have the bound

$$\phi_n \leq g_0 \exp\left(\sum_{m=0}^{n-1} k_m\right).$$

2.3 Entropy solutions

When working with weak solutions to hyperbolic conservation laws, we can often come into situations where there are several possible weak solutions. In these situations, we need a method of choosing which solution is "correct". Ideally, this would involve the use of some knowledge relating to the model in question. Often this means requiring the solution to be the limit of some diffusion equation. For a simple scalar hyperbolic equation, this typically starts by defining u^ε to be a solution to

$$\partial_t u^\varepsilon + \partial_x f(u^\varepsilon) = \partial_x^2 u^\varepsilon, \quad (2.2)$$

and then requiring

$$u = \lim_{\varepsilon \rightarrow 0} u^\varepsilon.$$

We look closer at this requirement for (1.4). Note that this section draws a lot from chapter 2.1 in [16], but with the source term added to the discussion.

Suppose then $u^\varepsilon = (u_1^\varepsilon, \dots, u_d^\varepsilon)$, is a solution to

$$\partial_t u_i^\varepsilon + \partial_x f_i(u_i^\varepsilon) = g_i(u^\varepsilon) + \varepsilon \partial_x^2 u_i^\varepsilon.$$

Then we multiply this by the derivative of a smooth convex function $\eta = \eta(u)$, and a positive test function ϕ , in $C_0^\infty(\mathbb{R} \times [0, T])$. Then we obtain

$$\begin{aligned} \iint g_i(u) \eta'(u_i^\varepsilon) \phi dx dt &= \iint (\partial_t u_i^\varepsilon + \partial_x f_i(u_i^\varepsilon) - \varepsilon \partial_x^2 u_i^\varepsilon) \eta'(u^\varepsilon) \phi dx dt \\ &= \iint \phi \partial_t \eta(u_i^\varepsilon) dx dt + \iint \phi \partial_x q(u_i^\varepsilon) dx dt \\ &\quad - \varepsilon \iint \partial_x^2 (\eta(u_i^\varepsilon) - \eta''(u_i^\varepsilon) (\partial_x u_i^\varepsilon)^2) \phi dx dt \\ &= \int_{\mathbb{R}} \eta(u_i^\varepsilon) \phi|_{t=T} dx - \int_{\mathbb{R}} \eta(u_i^\varepsilon) \phi|_{t=0} dx \\ &\quad - \iint \eta(u) \partial_t \phi dx dt - \iint q(u_i^\varepsilon) \partial_x \phi dx dt \\ &\quad - \varepsilon \iint \eta(u_i^\varepsilon) \partial_x^2 \phi dx dt + \varepsilon \iint \eta''(u_i^\varepsilon) (\partial_x u_i^\varepsilon)^2 \phi dx dt \\ &\geq \int_{\mathbb{R}} \eta(u_i^\varepsilon) \phi|_{t=T} dx - \int_{\mathbb{R}} \eta(u_i^\varepsilon) \phi|_{t=0} dx \\ &\quad - \iint (\eta(u_i^\varepsilon) \partial_t \phi + q(u_i^\varepsilon) \partial_x \phi + \varepsilon \eta(u_i^\varepsilon) \partial_x^2 \phi) dx dt \end{aligned}$$

where we define q such that

$$q'(u) = f'(u) \eta'(u). \quad (2.3)$$

The above argument stems from integration by parts, and the convexity of η , which gives $\eta'' \geq 0$. Thus we know $\eta''(u_i^\varepsilon) (\partial_x u_i^\varepsilon)^2 \phi \geq 0$.

We then let $\varepsilon \rightarrow 0$, giving the entropy inequality

$$\begin{aligned} \iint \eta(u_i) \partial_t \phi + q(u_i) \partial_x \phi - \int_{\mathbb{R}} \eta(u_i) \phi|_{t=T} dx + \int_{\mathbb{R}} \eta(u_i) \phi|_{t=0} dx \\ \geq - \iint g_i(u) \eta'(u_i) \phi dx dt. \end{aligned} \quad (2.4)$$

By certain density arguments it can be shown that it is sufficient if the above inequality holds for $\eta(u) = |u - k|$ for all real k . This gives $g(u) = \text{sgn}(u - k)(f(u) - f(k))$.

Finally, we note that in the case where we're looking for solutions on an infinite timescale, we'll use test functions in $C_0^\infty(\mathbb{R} \times [0, \infty))$, which allows us to remove the terminal conditions term from the entropy inequality.

2.4 Operator splitting

We give a short introduction to operator splitting as applied to the simpler equation

$$\partial_t u + \partial_x f(u) = g(u). \quad (2.5)$$

This is a scalar hyperbolic conservation law with a source term. One common technique for solving this problem is to split it into two steps.

Define first the operators $W(t)u_0$ and $R(t)u_0$ to denote the solutions at time t , for respectively

$$\partial_t u + \partial_x f(u) = 0,$$

and

$$\partial_t u = g(u).$$

Given $\Delta t > 0$, we then define the approximation sequence

$$u^0 = u_0, \quad u^{n+\frac{1}{2}} = W(\Delta t)u^n, \quad u^{n+1} = S(\Delta t)u^{n+\frac{1}{2}}. \quad (2.6)$$

We then use this sequence to define the approximate solution

$$u_{\Delta t}(x, t) = \begin{cases} W(2(t - t_n))u^n & \text{for } t \in [n\Delta t, (n + \frac{1}{2})\Delta t), \\ S(2(t - t_{n+\frac{1}{2}}))u^{n+\frac{1}{2}} & \text{for } t \in [(n + \frac{1}{2})\Delta t, (n + 1)\Delta t). \end{cases} \quad (2.7)$$

The next step would be to pick a sequence $\Delta t_k > 0$ converging to zero. Then use some compactness arguments to show that the family $u_{\Delta t_k}$, has some subsequence that will indeed converge to some function, u . Finally, we would aim to prove that u is indeed an entropy solution to (2.5). For a more thorough introduction to this topic, we refer to chapter 4 in [16] and for a comprehensive overview, we refer to [11].

2.5 Finite volume schemes

We will make good use of finite volume methods, applied to conservation laws of the form

$$\partial_t u + \partial_x f(u) = 0. \quad (2.8)$$

Much of this discussion is based on chapter three from [16]. For this, we need to apply a discretization, in space and in time. For this discretization, let $\Delta x > 0$, and $\Delta t > 0$. Then we discretize the axes by using node points $(x_j, t^n) = (j\Delta x, n\Delta t)$. We further give the useful definition $x_{j\pm\frac{1}{2}} = x_j \pm \frac{\Delta x}{2}$.

The next step is to find a numerical approximation at each point. For this, we will use the notation

$$u^{j,n} = \tilde{u}(j\Delta x, n\Delta t) \approx u(j\Delta x, n\Delta t) = u(x_j, t^n). \quad (2.9)$$

We will also use the notation, $u^n = \{u^{j,n}\}$ to denote the entire solution at the n th step in time. When handling the theory here we will use $j \in \mathbb{Z}$, so that the entire real line can be used. This

is of course not feasible to implement numerically. For implementation, one would need to use a bounded domain with suitable boundary conditions.

The approximate solution is often found based on some explicit rule of the form

$$u^{n+1} = G(u^n, \dots, u^{n-l}).$$

We say that the method is conservative if it can be written in the form

$$u^{j,n+1} = u^{j,n} - \lambda (F(u^{j-p,n}, \dots, u^{j+q,n}) - F(u^{j-p-1,n}, \dots, u^{j+q-1,n})), \quad (2.10)$$

where $\lambda = \frac{\Delta t}{\Delta x}$. We further say that the method is consistent if $F(c, \dots, c) = f(c)$. When working with hyperbolic systems we often meet the famous Courant-Friedrichs-Lewy (CFL) condition, which is stated as

$$\Delta t \max_s |f'(s)| \leq \Delta x. \quad (2.11)$$

We now take a short look at how a general finite volume method is constructed for (2.8). We first define the interval $I_j = [x_{j-\frac{1}{2}}, x_{j+\frac{1}{2}})$, and the cell $I_j^n = I_j \times [t^n, t^{n+1})$. We can integrate (2.8) over I_j to find that

$$\frac{d}{dt} \int_{I_j} u(x, t) dx = f(u(x_{j-\frac{1}{2}}, t)) - f(u(x_{j+\frac{1}{2}}, t)).$$

Finally, we can integrate in time as well to obtain the result

$$\int_{I_j} u(x, t^{n+1}) dx = \int_{I_j} u(x, t^n) dx + \int_{t^n}^{t^{n+1}} (f(u(x_{j-\frac{1}{2}}, t)) - f(u(x_{j+\frac{1}{2}}, t))) dt.$$

This gives the foundation for finite volume methods, where we aim to construct a method such that

$$F_i^{j+\frac{1}{2}}(u_i^n) \approx \frac{1}{\Delta x} \int_{t^n}^{t^{n+1}} f(u_i(x_{j+\frac{1}{2}}, t)) dt.$$

We now finish this discussion with some definitions which will see use later on.

Definition 2.1. Let $u_{\Delta t}$ be computed from a conservative and consistent method.

(i) A method is said to be monotone if for the initial data u^0 and v^0 , we have

$$u^{j,0} \leq v^{j,0}, \quad j \in \mathbb{Z} \implies u^{j,n} \leq v^{j,n}, \quad j \in \mathbb{Z}, n \in \mathbb{N}.$$

(ii) Assume that $u_0 \in L^1(\mathbb{R})$. Let $v_{\Delta t}$ be another solution with initial data $v_0 \in L^1(\mathbb{R})$. A numerical method is called L^1 contractive if

$$\|u_{\Delta t}(t) - v_{\Delta t}(t)\|_{L^1} \leq \|u_{\Delta t}(0) - v_{\Delta t}(0)\|_{L^1}$$

(iii) A method is said to be monotonicity preserving if given monotone initial data, u^n will also be monotone for all $n \in \mathbb{N}$.

The following theorem is very useful in showing properties of numerical schemes, and can be found in Theorem 3.6 from [16].

Theorem 2.4. For conservative and consistent methods the following hold:

(i) Assume initial data is integrable. In that case, every monotone method is L^1 -contractive.

(ii) Every L^1 -contractive method is TVD.

(iii) Every TVD method is monotonicity preserving.

3 Results for numerical schemes

In this section we establish the general numerical method, to be applied to weakly coupled systems of conservation laws on the form

$$\partial_t u_1 + \partial_x(f_1(u_1)) = S_1(u), \quad u_1(x, 0) = u_{1,0}(x), \quad (3.1a)$$

...

$$\partial_t u_d + \partial_x(f_d(u_d)) = S_d(u), \quad u_d(x, 0) = u_{d,0}(x). \quad (3.1b)$$

Here we will denote $S(u) = (S_1(u), \dots, S_d(u))$, and we will assume this source function to be Lipschitz. We also assume $f_i(u_i)$ to be Lipschitz continuous functions. As stated in the introduction, we will now apply operator splitting to solve this problem. The topic of operator splitting on weakly coupled conservation laws is not new and is explored thoroughly in the context of a more abstract framework in [11]. Here we instead take a more direct route, proving convergence to an entropy solution without the abstract framework of operator splitting used in [11].

We start by defining $W(t)(u_0)$ and $R(t)(u_0)$ to denote the solutions of respectively

$$\partial_t u_1 + \partial_x(f_1(u_1)) = 0, \quad u_1(x, 0) = u_{1,0}(x), \quad (3.2a)$$

...

$$\partial_t u_n + \partial_x(f_n(u_n)) = 0, \quad u_n(x, 0) = u_{n,0}(x), \quad (3.2b)$$

and

$$\partial_t u = S(u), \quad u(x, 0) = u_0(x). \quad (3.3)$$

Assuming the initial data to be integrable and of bounded variation, each of these gives a well-defined solution. Next, we go one step further, and let $W_{\Delta t}(t)(u_0)$ be an approximate solution operator for a finite volume scheme applied to (3.2), where Δt is a discretization parameter. Let also $R_{\Delta t}(t)(u_0)$ be the approximate solution operator for (3.3), with a standard forward Euler scheme. Note that the finite volume scheme would employ a spatial discretization parameter, Δx , in addition to Δt . However, we suppose this is calculated from Δt based on the CFL-condition, so we need only include Δt in the subscript.

Define also the operators

$$G(u) = W_{\Delta t}(\Delta t)(u), \quad \text{and} \quad H(u) = R_{\Delta t}(\Delta t)(u). \quad (3.4)$$

We can then state the resulting operator splitting scheme explicitly as

$$u_i^{j,n+\frac{1}{2}} = G_i^j(u_i^n) = u_i^{j,n} - \lambda(F_i^{j+\frac{1}{2},n} - F_i^{j-\frac{1}{2},n}), \quad (3.5)$$

$$u^{n+1} = H(u^{n+\frac{1}{2}}) = u^{n+\frac{1}{2}} + \Delta t S((u^{n+\frac{1}{2}})). \quad (3.6)$$

Here we have used the shorthand $F_i^{j+\frac{1}{2},n} = F_i(u_i^{j-p,n}, \dots, u_i^{j+q,n})$, and $\lambda = \frac{\Delta t}{\Delta x}$. The first half-step here is then a conservative scheme applied to (3.2), which we refer to as the flux step. While the second half-step here is an approximation to the solution of (3.3) and will be referred to as the source step. Having established this scheme we will use the next section to give a proof of convergence to an entropy solution.

We add a short remark on notation here. The indexing is in principle the same as established in the previous section regarding finite volume schemes, except for the new subscript which is due to the multi-dimensionality of (3.1). Stated directly this means we use the approximation

$$u_i^{j,n} \approx u_i(j\Delta x, n\Delta t).$$

3.1 Convergence results

We now aim to show that the generic type of scheme which has been described will indeed converge to an entropy solution of (3.1). We start this off by defining the function that we will use to approximate the final solution u ,

$$u^{\Delta t}(x, t) = \begin{cases} w^{j,n}, & (x, t) \in [x_{j-\frac{1}{2}}, x_{j+\frac{1}{2}}) \times [t^n, t^{n+\frac{1}{2}}), \\ w^{j,n+\frac{1}{2}}, & (x, t) \in [x_{j-\frac{1}{2}}, x_{j+\frac{1}{2}}) \times [t^{n+\frac{1}{2}}, t^{n+1}). \end{cases} \quad (3.7)$$

Before we look at convergence, we provide the following lemma.

Theorem 3.1. *Suppose $u_i^{\Delta t}$ is computed by an operator splitting as described above, where the flux step is computed by a conservative, consistent, and monotone scheme. Given a $u_{i,0}$ with bounded total variation, the total variation in space of $u_i^{\Delta t}(x, t)$ will be uniformly bounded for $t \in [0, T]$, with the bound depending only on T .*

We remark that the proof of this is inspired by the proof of Lemma 4.13 from [16], but in a discrete version.

Proof. We start by noting that the flux step is TVD due to 2.4. Thus we need only concern ourselves with the source step. Let $w_i^{j,n} = u_i^{j,n} - u_i^{j-1,n}$. Then we have

$$\begin{aligned} |w_i^{j,n+1}| &= \left| w_i^{j,n+\frac{1}{2}} + \Delta t (S_i^j(u^n) - S_i^{j-1}(u^n)) \right| \\ &\leq \left| w_i^{j,n+\frac{1}{2}} \right| + \Delta t \|S_i\|_{Lip} \sum_{k=1}^d \left| w_k^{j,n+\frac{1}{2}} \right| \\ &\leq \left(1 + \Delta t \|S_i\|_{Lip} \right) \left| w_i^{j,n+\frac{1}{2}} \right| + \Delta t \|S_i\|_{Lip} \sum_{k \neq i} \left| w_k^{j,n+\frac{1}{2}} \right|. \end{aligned}$$

Under the assumption that $\text{T.V.}(u_i^{n+\frac{1}{2}})$ is finite for every i , we can switch around the order of the sums and obtain:

$$\begin{aligned} \text{T.V.}(u_i^{n+1}) &= \sum_j |w_i^{j,n+1}| \\ &\leq (1 + \Delta t \|S_i\|_{Lip}) \sum_j \left| w_i^{j,n+\frac{1}{2}} \right| + \Delta t \|S_i\|_{Lip} \sum_{k \neq i} \sum_j \left| w_k^{j,n+\frac{1}{2}} \right| \\ &= (1 + \Delta t \|S_i\|_{Lip}) \text{T.V.}(u_i^{n+\frac{1}{2}}) + \Delta t \|S_i\|_{Lip} \sum_{k \neq i} \text{T.V.}(u_k^{n+\frac{1}{2}}) \\ &\leq (1 + d\Delta t) \max_k (\|S_k\|_{Lip} \text{T.V.}(u_k^{n+\frac{1}{2}})). \end{aligned}$$

We can then apply this inequality recursively together with the TVD property of the flux step to obtain

$$\max_k \text{T.V.}(u_k^n) \leq \max_k \text{T.V.}(u_k^0) + \sum_{m=0}^{n-1} (d\Delta t \max_k \|S_k\|_{Lip}) \max_k \text{T.V.}(u_k^m).$$

Thus we have a sequence of bounds to which we can apply the discrete Gronwall inequality, which gives

$$\begin{aligned}
\text{T.V.}(u_i^{\Delta t}(\cdot, t)) &= \text{T.V.}(u_i^n) \leq \max_k \text{T.V.}(u_k^n) \\
&\leq \max_k \text{T.V.}(u_k^0) \exp\left(\sum_{m=0}^{n-1} (d\Delta t \max_k \|S_k\|_{Lip})\right) \\
&= \max_k \text{T.V.}(u_k^0) \exp\left(d \max_k \|S_k\|_{Lip} t_n\right) \\
&\leq \max_k \text{T.V.}(u_k^0) \exp\left(d \max_k \|S_k\|_{Lip} T\right).
\end{aligned}$$

Thus we can conclude that for initial data with bounded total variation, the solution will have bounded total variation at any time $t \in [0, T]$. \square

With this bound on the total variation established, we have all we need to start proving some convergence theorems. We start by proving that given some sequence $\Delta t_k, \Delta x_k$, we get a subsequence converging to some weak solution. We also remark that much of this proof is similar to the proofs of theorems 3.4 and 3.8 in [16], but with the added technicality of the source step.

Theorem 3.2. *Fix $T > 0$. Assume that f is Lipschitz continuous. Let $u_{i,0} \in L^1(\mathbb{R})$ have bounded variation. Assume that $u^{\Delta t}$ is computed with a method as described above where the flux steps are consistent and conservative, and the source step is a forward Euler scheme. Assume also that the method is uniformly bounded, and of uniformly bounded total spatial variation, meaning*

$$\max_i \|u_i^{\Delta t}\|_{\infty} \leq M, \quad \text{and} \quad \max_{k,t} \text{T.V.} u_k^{\Delta t}(\cdot, t) \leq M, \quad (3.8)$$

where M is independent of Δx , and Δt . Then $\{u_i^{\Delta t_k}(t)\}$ has a subsequence that converges for all $t \in [0, T]$ to some $u(t) \in L^1_{loc}(\mathbb{R})$. Furthermore, the limit is in $C([0, T]; L^1_{loc}(\mathbb{R}))$, and is a weak solution to (3.1).

Proof. We will use 2.2 to prove convergence. The first two requirements are satisfied by (3.8). Thus we need only prove that

$$\int_{\mathbb{R}} |u_i^{\Delta t}(x, t) - u_i^{\Delta t}(x, s)| dx \leq C|s - t|, \quad \text{as } \Delta t \rightarrow 0.$$

We first note that

$$\begin{aligned}
|u_i^{j, n+\frac{1}{2}} - u_i^{j, n}| &\leq \lambda |F_i^{j+\frac{1}{2}, n} - F_i^{j-\frac{1}{2}, n}| \\
&\leq \lambda L (|u_i^{j-p, n} - u_i^{j-p-1, n}| + \dots + |u_i^{j+q, n} - u_i^{j+q-1, n}|).
\end{aligned}$$

Where L is the Lipschitz constant of F_i . We can use this to get the result that

$$\begin{aligned}
\left\| u_i^{\Delta t}(\cdot, t^n) - u_i^{\Delta t}(\cdot, t^{n+\frac{1}{2}}) \right\|_{L^1} &\leq \sum_j |u_i^{j, n+\frac{1}{2}} - u_i^{j, n}| \Delta x \\
&\leq \sum_j \Delta x \lambda L (|u_i^{j-p, n} - u_i^{j-p-1, n}| + \dots + |u_i^{j+q, n} - u_i^{j+q-1, n}|) \\
&\leq \Delta t L (p + q + 1) \sum_j |u_i^{j, n} - u_i^{j-1, n}| \leq \Delta t L (p + q + 1) M.
\end{aligned}$$

We next establish a bound on the change from the source step,

$$\left| u_i^{j,n+1} - u_i^{j,n+\frac{1}{2}} \right| = \Delta t \left| S_i(u^{j,n+\frac{1}{2}}) \right| \leq \Delta t \max_k \left| S_i(u^{k,n+\frac{1}{2}}) \right| \leq \Delta t C_H.$$

Where we define $C_H = \sup_{k,m,i} |S_i(u^{k,m})|$, which we know to be bounded due to (3.8). Thus we can obtain the following:

$$\|u_{\Delta t,i}(\cdot, t^p) - u_{\Delta t,i}(\cdot, t^q)\|_{L^1} \leq (C_H + L(p+q+1)M)|t^p - t^q|.$$

We need to do a short argument here to expand the inequality to include times not on the exact discretization times, t^n . Let $t_1, t_2 \in [0, T]$, and pick two times $\tau_1, \tau_2 \in \{n\frac{\Delta t}{2} | 0 \leq n \leq T/\Delta t\}$ such that

$$0 \leq t_j - \tau_j < \Delta t \text{ for } j = 1, 2.$$

Then we know $u^{\Delta t}(t_j) = u^{\Delta t}(\tau_j)$, so

$$\begin{aligned} \|u_i^{\Delta t}(\cdot, t_1) - u_i^{\Delta t}(\cdot, t_2)\|_{L^1} &\leq \|u_i^{\Delta t}(\cdot, \tau_1) - u_i^{\Delta t}(\cdot, \tau_2)\|_{L^1} \\ &\leq (C_H + L(p+q+1)M)|\tau_2 - \tau_1| \\ &\leq (C_H + L(p+q+1)M)|t_2 - t_1| + \mathcal{O}(\Delta t). \end{aligned}$$

Thus we conclude that there exists some subsequence such that $u_i^{\Delta t_k} \rightarrow u_i$ in $C([0, T]; L^1(\mathbb{R}))$. We next show that this furthermore need be a weak solution. We start from the definition of the flux step,

$$u_i^{j,n+\frac{1}{2}} - u_i^{j,n} = \lambda(F_i^{j-\frac{1}{2},n} - F_i^{j+\frac{1}{2},n}).$$

Let φ be some test function, and let $\varphi_j^n = \varphi(x_j, t^n)$. We multiply this by $\varphi_j^n \Delta x$, and sum over j to get

$$\sum_j (u_i^{j,n+\frac{1}{2}} - u_i^{j,n}) \varphi_j^n \Delta x = \lambda \sum_j (F_i^{j-\frac{1}{2},n} - F_i^{j+\frac{1}{2},n}) \varphi_j^n \Delta x.$$

We do some partial summation tricks here to get

$$\begin{aligned} \sum_j (u_i^{j,n+\frac{1}{2}} - u_i^{j,n}) \varphi_j^n \Delta x &= \sum_j u_i^{j,n+\frac{1}{2}} \left(\frac{\varphi_j^n - \varphi_j^{n+\frac{1}{2}}}{\Delta t/2} \right) \Delta x \Delta t/2 \\ &\quad + \sum_j u_i^{j,n+\frac{1}{2}} \varphi_j^{n+\frac{1}{2}} \Delta x - \sum_j u_i^{j,n} \varphi_j^n \Delta x, \end{aligned}$$

and

$$\sum_j (F_i^{j+\frac{1}{2},n} - F_i^{j-\frac{1}{2},n}) \lambda \varphi_j^n \Delta x = \sum_j F_i^{j+\frac{1}{2},n} \left(\frac{\varphi_j^n - \varphi_{j+1}^n}{\Delta x} \right) \Delta x \Delta t.$$

Next we take a look at the source term, again summing over j and multiplying by $\varphi_j^{n+\frac{1}{2}} \Delta x$.

$$\sum_j (u_i^{j,n+1} - u_i^{j,n+\frac{1}{2}}) \varphi_j^{n+\frac{1}{2}} \Delta x = \sum_j S_i(u^{j,n+\frac{1}{2}}) \varphi_j^{n+\frac{1}{2}} \Delta t \Delta x.$$

Where we can do the same trick with partial summation as before to the left-hand side. Combining this with the equality from the flux step, and summing over n , we get

$$\begin{aligned}
& \sum_{j,n} u_i^{j,n+\frac{1}{2}} \left(\frac{\varphi_j^n - \varphi_j^{n+\frac{1}{2}}}{\Delta t/2} \right) \Delta x \Delta t/2 + u_i^{j,n+1} \left(\frac{\varphi_j^{n+\frac{1}{2}} - \varphi_j^{n+1}}{\Delta t/2} \right) \Delta x \Delta t/2 \\
& \quad + \sum_j u_i^{j,N} \varphi_j^N \Delta x - \sum_j u_i^{j,0} \varphi_j^0 \Delta x \\
& \quad + \sum_{j,n} F_i^{j+\frac{1}{2},n} \left(\frac{\varphi_j^n - \varphi_{j+1}^n}{\Delta x} \right) \Delta x \Delta t \\
& = \sum_{j,n} S_i(u^{j,n+\frac{1}{2}}) \varphi_j^{n+\frac{1}{2}} \Delta t \Delta x.
\end{aligned}$$

We are now left only with the task of showing the following convergences:

$$\sum_{j,n} u_i^{j,n/2} \left(\frac{\varphi_j^{(n+1)/2} - \varphi_j^{n/2}}{\Delta t/2} \right) \Delta x \Delta t/2 \rightarrow \int_0^T \int_{\mathbb{R}} u_i \partial_t \varphi dx dt, \quad (3.9a)$$

$$\sum_j u_i^{j,N} \varphi_j^N \Delta x - \sum_j u_i^{j,0} \varphi_j^0 \Delta x \rightarrow \int_{\mathbb{R}} u_i \varphi|_0^T dx, \quad (3.9b)$$

$$\sum_{j,n} F_i^{j+\frac{1}{2},n} \left(\frac{\varphi_j^n - \varphi_{j+1}^n}{\Delta x} \right) \Delta x \Delta t \rightarrow \int_0^T \int_{\mathbb{R}} f_i(u_i) \partial_x \varphi dx dt, \quad (3.9c)$$

$$\sum_j S_i(u^{j,n+\frac{1}{2}}) \varphi_j^{n+\frac{1}{2}} \Delta t \Delta x \rightarrow \int_0^T S_i(u) \varphi dx dt. \quad (3.9d)$$

We will show the convergence of (3.9c), and remark that the convergence of the remaining terms can be shown in a similar manner. We note that due to the compact support of φ , and the assumed boundedness of $u^{\Delta t}$, we can use a constant function as the dominating function in Lebesgue dominated convergence theorem. Thus we may freely switch any limits and sums. We can also perform a more detailed proof, starting with

$$\begin{aligned}
& \left| \int_0^T \int_{\mathbb{R}} f_i(u_i) \partial_x \varphi dx dt - \sum_{j,n} F_i^{j+\frac{1}{2},n} \left(\frac{\varphi_{j+1}^n - \varphi_j^n}{\Delta x} \right) \Delta x \Delta t \right| \\
& \leq \sum_{j,n} \left| \iint_{I_j^n} f_i(u_i) \partial_x \varphi dx dt - F_i^{j+\frac{1}{2},n} \left(\frac{\varphi_{j+1}^n - \varphi_j^n}{\Delta x} \right) \Delta x \Delta t \right|.
\end{aligned}$$

We start by putting focus on a single of these terms.

$$\begin{aligned}
& \left| \iint_{I_j^n} f_i(u_i) \partial_x \varphi dx dt - F_i^{j+\frac{1}{2},n} \left(\frac{\varphi_{j+1}^n - \varphi_j^n}{\Delta x} \right) \Delta x \Delta t \right| \\
& \leq \iint_{I_j^n} \left| f_i(u_i) \partial_x \varphi - f_i(u_i) \frac{\varphi_{j+1}^n - \varphi_j^n}{\Delta x} \right| dx dt \\
& + \iint_{I_j^n} \left| f_i(u_i) \left(\frac{\varphi_{j+1}^n - \varphi_j^n}{\Delta x} \right) - F_i^{j+\frac{1}{2},n} \left(\frac{\varphi_{j+1}^n - \varphi_j^n}{\Delta x} \right) \right| dx dt \\
& \leq \iint_{I_j^n} |f_i(u_i)| dx dt \left\| \varphi_x - \frac{\varphi_{j+1}^n - \varphi_j^n}{\Delta x} \right\|_\infty \\
& + \left\| \frac{\varphi_{j+1}^n - \varphi_j^n}{\Delta x} \right\|_\infty \iint_{I_j^n} |f_i(u_i) - F_i^{j+\frac{1}{2},n}| dx dt \\
& \leq \iint_{I_j^n} |f_i(u_i)| dx dt \left\| \varphi_x - \frac{\varphi_{j+1}^n - \varphi_j^n}{\Delta x} \right\|_\infty \\
& + \left\| \frac{\varphi_{j+1}^n - \varphi_j^n}{\Delta x} \right\|_\infty \left(\iint_{I_j^n} |f_i(u_i) - f_i(u_i^{j+\frac{1}{2},n})| + |f_i(u_i^{j+\frac{1}{2},n}) - F_i^{j+\frac{1}{2},n}| dx dt \right).
\end{aligned}$$

We focus furthermore on the last term,

$$\begin{aligned}
\iint_{I_j^n} |f_i(u_i^{j,n}) - F_i^{j+\frac{1}{2},n}| dx dt & = |F_i(u_i^{j,n}, \dots, u_i^{j,n}) - F_i(u_i^{j-p,n}, \dots, u_i^{j+q,n})| \Delta t \Delta x \\
& \leq \|F_i\|_{Lip} (|u_i^{j-p,n} - u_i^{j,n}| + \dots + |u_i^{j+q,n} - u_i^{j,n}|) \Delta t \Delta x.
\end{aligned}$$

We can then apply the compact support of φ to sum over only a finite list of indices between A, B in j . Such that $\text{supp } \varphi \subset [a, b] \times [0, T] \subset [A\Delta x, B\Delta x] \times [0, T]$. Then we conclude with the following bound

$$\begin{aligned}
& \left| \int_0^T \int_{\mathbb{R}} f_i(u_i) \partial_x \varphi dx dt - \sum_{j,n} F_i^{j+\frac{1}{2},n} \left(\frac{\varphi_{j+1}^n - \varphi_j^n}{\Delta x} \right) \Delta x \Delta t \right| \\
& \leq \max_{k,m} \max_{(\bar{x}, \bar{t}) \in I_k^m} \left| \varphi_x((\bar{x}, \bar{t})) - \left(\frac{\varphi_{k+1}^m - \varphi_k^m}{\Delta x} \right) \right| \int_0^T \int_a^b |f_i(u_i)| dx dt \\
& + \max_{k,m} \left| \frac{\varphi_{k+1}^m - \varphi_k^m}{\Delta x} \right| \int_0^T \int_a^b |f_i(u_i) - f_i(u_i^{\Delta t})| dx dt \\
& + \max_{k,m} \left| \frac{\varphi_{k+1}^m - \varphi_k^m}{\Delta x} \right| \left(\sum_{n=0}^{N-1} \sum_{j=A}^B \|F_i\|_{Lip} (|u_i^{j-p,n} - u_i^{j,n}| + \dots + |u_i^{j+q,n} - u_i^{j,n}|) \right) \Delta t \Delta x.
\end{aligned}$$

Letting $\Delta t \rightarrow 0$, $\Delta x \rightarrow 0$, the first term goes to zero due to the smoothness of φ , the second term goes to zero due to the Lipschitz continuity of f_i and the convergence of $u_i^{\Delta t} \rightarrow u_i$. For the final term, we note the bound

$$\sum_{j=A}^B \|F_i\|_{Lip} (|u_i^{j-p,n} - u_i^{j,n}| + \dots + |u_i^{j+q,n} - u_i^{j,n}|) \leq \|F_i\|_{Lip} (p+q+1) \text{T.V.}(u_i^{\Delta t}).$$

Which we again know to have an upper bound. Thus the last term also goes to zero as $\Delta x \rightarrow 0$. We again remark that the convergence of the other terms in (3.9) can be done by similar methods.

Thus we conclude that u is indeed a weak solution to (3.1). \square

We finish this discussion of convergence by showing that the sequence of approximate solutions will converge to an entropy solution. We first recall that u is an entropy solution to (3.1) if

$$\begin{aligned} \iint |u_i - k| \partial_t \phi + \operatorname{sgn}(u_i - k) (f_i(u_i) - f_i(k)) \partial_x \phi - \int_{\mathbb{R}} |u_i - k| \phi|_{t=T} dx + \int_{\mathbb{R}} |u_i - k| \phi|_{t=0} dx \\ \geq - \iint S_i(u) \operatorname{sgn}(u_i - k) \phi dx dt. \end{aligned} \quad (3.10)$$

In order to prove that the element of convergence is indeed an entropy solution, we first need to define the numerical entropy flux, which is defined as $Q_i^{j+\frac{1}{2},n}(u) = F_i^{j+\frac{1}{2},n}(u \vee k) - F_i^{j+\frac{1}{2},n}(u \wedge k)$, where we note that $Q_i(c, \dots, c) = \operatorname{sgn}(c - k) (f_i(c) - f_i(k))$. We now state the concluding theorem of this section. We remark here that this proof is similar to the proofs of Theorem 3.9, and Theorem 4.14 from [16].

Theorem 3.3. *Fix $T > 0$. Let $u_{i,0} \in L^1(\mathbb{R})$ have bounded variation. Let $\{\Delta t_k\}$, and $\{\Delta x_k\}$ be positive sequences converging to zero such that $\lambda = \frac{\Delta t_k}{\Delta x_k}$ satisfies the CFL conditions. Then let $u^{\Delta t_k}$ be calculated by a scheme as we have previously described. Given that the flux step is calculated by a conservative, consistent, and monotone scheme, and $u^{\Delta t_k}$ is uniformly bounded, meaning*

$$\max_i \|u_i^{\Delta t}\|_{\infty} \leq M, \quad (3.11)$$

where M is a constant independent of Δt . Then $u^{\Delta t_k}$ converges to $u \in C([0, \infty); L^1(\mathbb{R}))$ which is an entropy solution to (3.1).

Proof. Combining the monotonicity of the flux step with 3.1 we get that all the assumptions of 3.2 hold. Thus the previous discussion gives us at once convergence to a weak solution. Thus it remains only to show that this is also an entropy solution.

We start by noting that the monotonicity of the flux step gives the inequality

$$\left| u_i^{j,n+\frac{1}{2}} - k \right| - \left| u_i^{j,n} - k \right| + \lambda (Q_i^{j+\frac{1}{2},n} - Q_i^{j-\frac{1}{2},n}) \leq 0.$$

Let φ be a positive test function. Multiplying by $\varphi_j^n \Delta x$, summing over j , and performing some similar tricks to those used before we get the inequality

$$\begin{aligned} \sum_j \left(\frac{\varphi_j^{n+\frac{1}{2}} - \varphi_j^n}{\Delta t} \right) \left| u_i^{j+\frac{1}{2}} - k \right| \Delta x \Delta t + \sum_j Q_i^{j+\frac{1}{2},n} \left(\frac{\varphi_{j+1}^n - \varphi_j^n}{\Delta x} \right) \Delta x \Delta t \\ + \sum_j \left(\left| u_i^{j,n} - k \right| \varphi_j^n - \left| u_i^{j,n+\frac{1}{2}} - k \right| \varphi_j^{n+\frac{1}{2}} \right) \Delta x \geq 0. \end{aligned}$$

We next take a closer look at the source step. Here we have

$$\begin{aligned} \left| u_i^{j,n+1} - k \right| - \left| u_i^{j,n+\frac{1}{2}} - k \right| &= \left| u_i^{j,n+\frac{1}{2}} + \Delta t S_i(u^{j,n+\frac{1}{2}}) - k \right| - \left| u_i^{j,n+\frac{1}{2}} - k \right| \\ &= (u_i^{j,n+\frac{1}{2}} - k) \left(\operatorname{sgn}(u_i^{j,n+1} - k) - \operatorname{sgn}(u_i^{j,n+\frac{1}{2}} - k) \right) \\ &\quad + \Delta t \operatorname{sgn}(u_i^{j,n+1}) S_i(u^{j,n+\frac{1}{2}}). \end{aligned}$$

Performing similar tricks as in the proof of 3.2, multiplying by $\varphi_j^{n+\frac{1}{2}} \Delta x$, and rearranging terms from the sum we get

$$\begin{aligned} & \sum_j |u_i^{j,n+1} - k| \left(\frac{\varphi_j^{n+1} - \varphi_j^{n+\frac{1}{2}}}{\Delta t/2} \right) \frac{\Delta t}{2} \Delta x - \sum_j |u_i^{j,n+1} - k| \varphi_j^{n+1} \Delta x + \sum_j |u_i^{j,n+\frac{1}{2}} - k| \varphi_j^{n+\frac{1}{2}} \Delta x \\ &= - \sum_j \operatorname{sgn}(u_i^{j,n+1} - k) S_i(u^{j,n+\frac{1}{2}}) \Delta t \Delta x \\ & \quad + \sum_j (u_i^{j,n+\frac{1}{2}} - k) (\operatorname{sgn}(u_i^{j,n+1} - k) - \operatorname{sgn}(u_i^{j,n+\frac{1}{2}} - k)) \Delta x. \end{aligned}$$

We can then combine the flux step and the source step to obtain

$$\begin{aligned} & \sum_{j,n} |u_i^{j,n+1-k}| \left(\frac{\varphi_j^{n+1} - \varphi_j^{n+\frac{1}{2}}}{\Delta t/2} \right) \frac{\Delta t}{2} \Delta x + \sum_{j,n} |u_i^{j,n+\frac{1}{2}-k}| \left(\frac{\varphi_j^{n+\frac{1}{2}} - \varphi_j^n}{\Delta t/2} \right) \frac{\Delta t}{2} \Delta x \\ & + \sum_j |u_i^{j,0} - k| \varphi_j^0 \Delta x - \sum_j |u_i^{j,N} - k| \varphi_j^N \Delta x \\ & + \sum_{j,n} Q_i^{j+\frac{1}{2},n} \left(\frac{\varphi_{j+1}^n - \varphi_j^n}{\Delta x} \right) \Delta x \Delta t \\ & \geq - \sum_{j,n} \operatorname{sgn}(u_i^{j,n+1} - k) S_i(u^{j,n+\frac{1}{2}}) \varphi_j^{n+\frac{1}{2}} \Delta x \Delta t \\ & \quad - \sum_{j,n} (u_i^{j,n+\frac{1}{2}} - k) (\operatorname{sgn}(u_i^{j,n+1} - k) - \operatorname{sgn}(u_i^{j,n+\frac{1}{2}} - k)) \Delta x. \end{aligned}$$

We use the following observation to justify the final inequality

$$(u_i^{j,n+\frac{1}{2}} - k) \left(\operatorname{sgn}(u_i^{j,n+1} - k) - \operatorname{sgn}(u_i^{j,n+\frac{1}{2}} - k) \right) = \begin{cases} -2 |u_i^{j,n+\frac{1}{2}} - k|, & \Delta_i^{j,n} \neq 0 \\ 0, & \Delta_i^{j,n} = 0, \end{cases} \quad (3.12)$$

which is easily found by looking at this term for the different possible cases of $\operatorname{sgn}(u_i^{j,n+1} - k) - \operatorname{sgn}(u_i^{j,n+\frac{1}{2}} - k)$. Finally, we observe that in the cases where $\operatorname{sgn}(u_i^{j,n+1} - k) \neq \operatorname{sgn}(u_i^{j,n+\frac{1}{2}} - k)$, we also must have the bound

$$|u_i^{j,n+\frac{1}{2}} - k| \leq \Delta t |S_i(u^{j,n+\frac{1}{2}})|.$$

Thus we can conclude that

$$\begin{aligned} & - \sum_{j,n} \operatorname{sgn}(u_i^{j,n+1} - k) S_i(u^{j,n+\frac{1}{2}}) \varphi_j^{n+\frac{1}{2}} \Delta x \Delta t \\ & - \sum_{j,n} (u_i^{j,n+\frac{1}{2}} - k) (\operatorname{sgn}(u_i^{j,n+1} - k) - \operatorname{sgn}(u_i^{j,n+\frac{1}{2}} - k)) \Delta x \\ & \geq - \sum_{j,n} \operatorname{sgn}(u_i^{j,n+1} - k) S_i(u^{j,n+\frac{1}{2}}) \varphi_j^{n+\frac{1}{2}} \Delta x \Delta t. \end{aligned}$$

With all this in place, we are only left with proving these convergences, and we are done.

$$\sum_{j,n} |u_i^{j,\frac{n+1}{2}} - k| \left(\frac{\varphi_j^{\frac{n+1}{2}} - \varphi_j^{n/2}}{\Delta t/2} \right) \frac{\Delta t}{2} \Delta x \rightarrow \int_0^T \int_{\mathbb{R}} |u_i - k| \varphi_t dx dt, \quad (3.13a)$$

$$\sum_j |u_i^{j,0} - k| \varphi_j^0 \Delta x - \sum_j |u_i^{j,N} - k| \varphi_j^N \Delta x \rightarrow \int_{\mathbb{R}} (|u_i - k| \varphi)|_{t=0}^T dx, \quad (3.13b)$$

$$\sum_{j,n} Q_i^{j+\frac{1}{2},n} \left(\frac{\varphi_{j+1}^n - \varphi_j^n}{\Delta x} \right) \Delta x \Delta t \rightarrow \int_0^T \int_{\mathbb{R}} \operatorname{sgn}(u_i - k) (f_i(u_i) - f_i(k)) \varphi_x dx dt, \quad (3.13c)$$

$$\sum_{j,n} \operatorname{sgn}(u_i^{j,n+1} - k) S_i(u^{j+\frac{1}{2}}) \varphi_j^{n+\frac{1}{2}} \Delta x \Delta t \rightarrow \int_0^T \int_{\mathbb{R}} \operatorname{sgn}(u_i - k) S_i(u) \varphi dx dt. \quad (3.13d)$$

Again, each of these can be proven in quite similar ways as the integrals converging at the end of the proof for the last theorem. Thus we can conclude that u is an entropy solution to (3.1). Finally, since the entropy solution is unique, and the above discussion gives that every convergent subsequence of $u^{\Delta t_k}$, will converge to an entropy solution to (3.1). Thus we can conclude that $u^{\Delta t_k}$ converges to the entropy solution itself. \square

4 Simulations on multilane traffic flow

In this section, we will utilize the numerical framework we have now established to analyze a model for multilane vehicular traffic. This model was presented in the introduction, see (1.2). However, for the benefit of the reader, we reintroduce the model here

$$\partial_t u_1 + \partial_x(u_1 v_1(u_1)) = -S(u_1, u_2), \quad u_1(x, 0) = u_{1,0}(x), \quad (4.1a)$$

$$\partial_t u_2 + \partial_x(u_2 v_2(u_2)) = S(u_1, u_2), \quad u_2(x, 0) = u_{2,0}(x), \quad (4.1b)$$

with

$$S(u_1, u_2) = (v_2(u_2) - v_1(u_1)) \begin{cases} u_1, & v_2(u_2) \geq v_1(u_1), \\ u_2, & v_2(u_2) < v_1(u_1). \end{cases} \quad (4.2)$$

The velocity functions can in general be any strictly decreasing continuously differentiable function, but for all simulations, we will restrict ourselves to Greenshield models for the velocity of vehicles. These models have their roots all their way back to the work of Greenshield in [8]. The general model for velocity is then

$$v(u) = v_{max}(1 - u^n)[0 \leq u \leq 1] + v_{max}[0 > u], \quad n \in \mathbb{N}. \quad (4.3)$$

Other models for the velocity do however exist, see [7] or exercise 2.2 in [16]. We note also the added complexities to flatten the velocity function for $u \notin [0, 1]$. These are not necessary for the analytical case, as Lemma 2.4 of [15], gives that for initial conditions contained in $[0, 1]$, the solution will stay in $[0, 1]$. However, in numerical simulations we may get timesteps in which the approximate solution is outside of $[0, 1]$. We will however suppress these parts of the definitions. In particular this means we will write down the definitions of the velocities as

$$v_1(u_1) = 1 - u_1^{n_1}, \quad v_2(u_2) = c(1 - u_2^{n_2}), \quad (4.4)$$

where c is some positive real number. We note that given two general velocity functions on the form (4.3) can always be rescaled to the latter form, see appendix A. We quickly note that a high value for n_i here means that the drivers will drive at close to the speed limit until there is a pretty high density of cars. You could then say that higher values of n_i mean that the drivers are better, or you could say this means the drivers are more reckless. Which of these you say should depend on how great n_i is, but where the limit goes is a topic of discussion. We also remark that the CFL condition becomes a lot stricter with higher values of n_i . In order to perform this analysis we start by presenting the specifics of our chosen finite volume scheme. Then we move on to present the results, together with some model interpretation of the results.

For our simulations, we utilize the Engquist-Osher flux for the finite volume step. The Engquist-Osher flux is defined as

$$f_i^{EO}(u, w) = \frac{1}{2}(f_i(u) + f_i(w) - \int_u^w |f_i'(s)| ds). \quad (4.5)$$

We write up the total scheme we will use for simulations:

$$u_i^{j, n+\frac{1}{2}} = u_i^{j, n} - \lambda (f_i^{EO}(u_i^{j, n}, u_i^{j+1, n}) - f_i^{EO}(u_i^{j-1, n}, u_i^{j, n})), \quad (4.6)$$

$$u_i^{j, n+1} = u_i^{j, n+\frac{1}{2}} + \Delta t (-1)^i S(u_1^{j, n+\frac{1}{2}}, u_2^{j, n+\frac{1}{2}}). \quad (4.7)$$

We see at once that this gives a conservative scheme, with the numerical flux

$$F_i^{j+\frac{1}{2}, n}(u_i) = f_i^{EO}(u_i^{j, n}, u_i^{j+1, n}).$$

For practical reasons, we will actually use somewhat different definitions, with

$$f_i(u_i) = \begin{cases} u_i v_i(u_i), & 0 \leq u_i \leq 1, \\ 0, & u_i \in (-\infty, 0) \cup (1, \infty) \end{cases} \quad (4.8)$$

and

$$S(u_1, u_2) = (v_2(u_2) - v_1(u_1)) \begin{cases} u_1^+, & v_2(u_2) \geq v_1(u_1), \\ u_2^+, & v_2(u_2) < v_1(u_1). \end{cases} \quad (4.9)$$

This redefinitions are solely there to make sure the numerical properties are as they should, when the approximation gives us densities outside of $[0, 1]$. These redefinitions will be implicitly assumed to be there later, when numerical proofs are done, but will be suppressed for the sake of niceness.

We will now present some useful properties of the Engquist-Osher scheme, showing that it satisfies the conditions necessary for 3.3.

4.1 The Engquist-Osher scheme

We now present the Engquist-Osher scheme, which was originally presented in [4], [5]. This scheme is well understood, and all the properties discussed here are also discussed in the original presentation. However, for the benefit of the reader, we include proofs for the properties most relevant to our discussion.

We first wish to show some fundamental properties of this scheme. We start by looking at properties of the flux approximation.

Lemma 4.1. *The Engquist-Osher flux function satisfies the following properties*

(i) *Lipschitz continuity, i.e. there exists some $L \in \mathbb{R}$ such that for any $u, w, x, y \in \mathbb{R}$ we have*

$$|f_i^{EO}(u, w) - f_i^{EO}(x, y)| \leq L(|u - x| + |w - y|)$$

(ii) *Consistency $f_i^{EO}(u, u) = f_i(u)$*

Proof. We prove (i) first, by doing the following simple chain of inequalities

$$\begin{aligned} |f_i^{EO}(u, w) - f_i^{EO}(x, y)| &\leq |f_i^{EO}(u, w) - f_i^{EO}(x, w)| + |f_i^{EO}(x, w) - f_i^{EO}(x, y)| \\ &\leq \|\partial_u f_i^{EO}\|_\infty |u - x| + \|\partial_w f_i^{EO}\|_\infty |w - y| \\ &\leq \|f_i'\|_\infty (|u - x| + |w - y|). \end{aligned}$$

Where $\partial_u f_i^{EO}$ denotes the partial derivative of f_i^{EO} with respect to the first variable, and $\partial_w f_i^{EO}$, with respect to the second variable. (ii) follows trivially by noting

$$f_i^{EO}(u, u) = \frac{1}{2}(f_i(u) + f_i(u) - \int_u^u |f'(s)| ds) = f_i(u).$$

□

Here we first aim to show that this method is indeed monotone, which we can do quite easily by taking partial derivatives. We first note the partial derivatives of the Engquist-Osher flux function

$$\begin{aligned} \partial_u(f_i^{EO}(u, w)) &= \frac{1}{2}(f_i'(u) + |f_i'(u)|) = (f_i'(u))^+, \\ \partial_w(f_i^{EO}(u, w)) &= \frac{1}{2}(f_i'(w) - |f_i'(w)|) = -(f_i'(w))^- \end{aligned}$$

With these established we can move on to taking the partial derivatives of the entire discretization

$$\begin{aligned}\frac{\partial u_i^{j,k+1}}{\partial u_i^{j+1,k}} &= -\lambda \partial_w f_i^{EO}(u_i^{j,k}, u_i^{j+1,k}) = \lambda (f_i'(u_i^{j+1,k}))^- \geq 0, \\ \frac{\partial u_i^{j,k+1}}{\partial u_i^{j-1,k}} &= \lambda \partial_u f_i^{EO}(u_i^{j-1,k}, u_i^{j,k}) = \lambda (f_i'(u_i^{j-1,k}))^+ \geq 0, \\ \frac{\partial u_i^{j,k+1}}{\partial u_i^{m,k}} &= 0, \quad \forall m \notin \{j-1, j, j+1\}.\end{aligned}$$

We are only left with taking the partial derivative with respect to $u_i^{j,k}$, which gives a derivative

$$\frac{\partial u_i^{j,k+1}}{\partial u_i^{j,k}} = 1 - \lambda (\partial_u f_i(u_i^{j,k}, u_i^{j+1,k}) - \partial_w f_i^{EO}(u_i^{j-1,k}, u_i^{j,k})) = 1 - \lambda |f_i'(u_i^{j,k})|.$$

Thus we can conclude that the Engquist-Osher scheme gives a monotone scheme in case we have

$$1 > \lambda |f_i'(s_i)|, \quad (4.10)$$

for all s_i , which is of course the CFL-condition.

Thus we can conclude that this is in fact a monotone scheme given that the CFL-condition is satisfied for all the lanes.

It is also necessary to check on the boundedness of $u^{\Delta t}$. We know from Lemma 2.4 in [15], that assuming initial data contained in $[0, 1]$, the solution of (4.1) will have range contained in $[0, 1]$. We thus wish to look into possible values of $u^{\Delta t}$ when computed with the Engquist-Osher scheme. Suppose first we have some $u_i^{j,n} \leq 0$. Since (4.8) guarantees $f_i \geq 0$ everywhere. Furthermore, we have $f_i(u_i^{j,n}) = 0$, which then gives

$$\begin{aligned}f_i^{EO}(u_i^{j,n}, u_i^{j+1,n}) &= \frac{1}{2} \left(f_i(u_i^{j+1,n}) - \int_0^{u_i^{j+1,n}} |f_i'(s)| ds \right) \leq 0, \\ f_i^{EO}(u_i^{j-1,n}, u_i^{j,n}) &= \frac{1}{2} \left(f_i(u_i^{j-1,n}) + \int_0^{u_i^{j-1,n}} |f_i'(s)| ds \right) \geq 0.\end{aligned}$$

Combining these into the actual scheme we see that

$$u_i^{j,n+\frac{1}{2}} \geq u_i^{j,n}.$$

Whenever $u_i^{j,n} \leq 0$. We can then do a similar argument to show that

$$u_i^{j,n+\frac{1}{2}} \leq u_i^{j,n}.$$

Whenever $u_i^{j,n} \geq 1$. Finally, due to the boundedness of f_i we can conclude that given initial data contained in $[0, 1]$, there exists some constant $M < \infty$, such that $u_i^{j,n+\frac{1}{2}} \in [0 - M, 1 + M]$. We can make very similar arguments for the source step to conclude that there exists some constant $M < \infty$ such that given initial data with $u_i^{j,0} \in [0 - M, 1 + M]$, we will have $u_i^{j,n/2} \in [0 - M, 1 + M]$. We can then conclude that our scheme satisfies all the requirements from 3.3.

We finish this section by mentioning the useful fact that given a concave flux function with a unique maxima at $u = \omega$, we have the formula

$$f_i^{EO}(u, v) = f_i(u \wedge \omega) + f_i(v \vee \omega) - f_i(\omega). \quad (4.11)$$

4.2 Simulation results

Now that we have established the most important properties of (4.6), we move on to do some simulations of (4.1).

We note that since we have restricted ourselves to Greensfield type velocity functions, we will also have concave flux functions. Thus we can utilize (4.11) for much faster simulations. All implementation and simulations were done in Python.

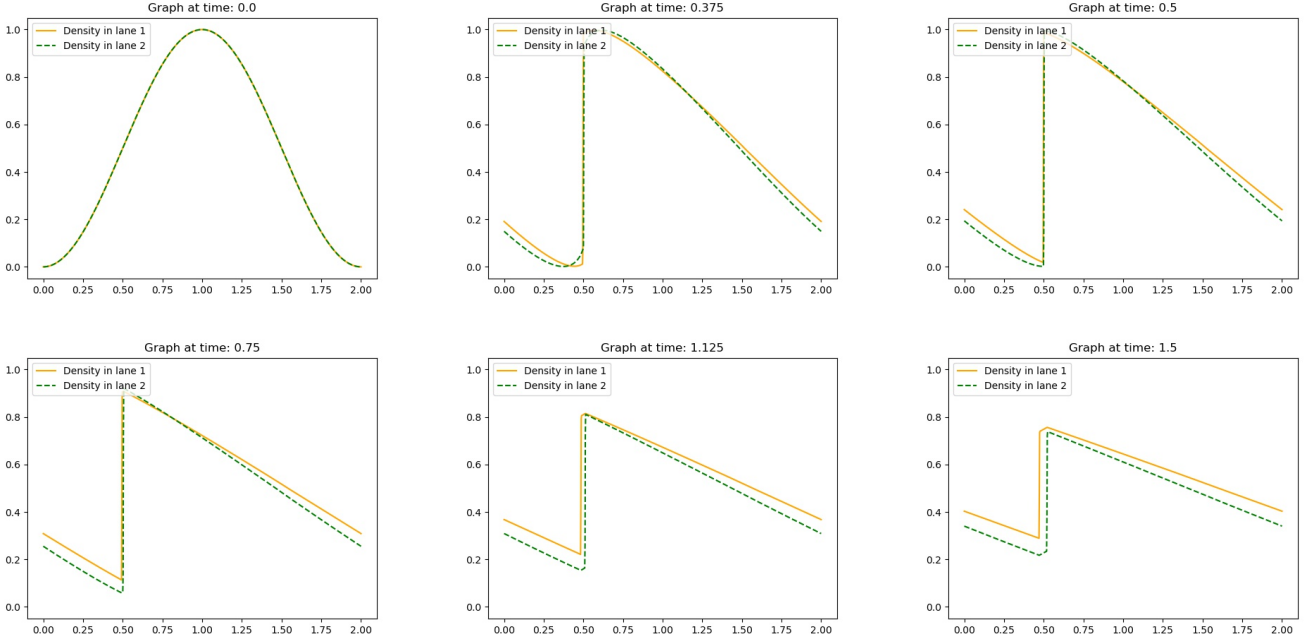


Figure 1: Results from simulations with lane configurations (4.12). The simulations were done using roads of length $l = 2$.

4.2.1 General behaviour with periodic boundary conditions

We start out looking for simple results regarding the expected behaviour of (4.1). To easily obtain some results regarding this behaviour we utilize periodic boundary conditions in this section, meaning that

$$u(0, t) = u(l, t), \quad \forall t.$$

In this case, we must be careful to assume that observed behaviour can be generalized to solutions on the entire real line, as any behaviour we observe might come from boundary effects.

We begin with a simple case where we have velocity functions and initial conditions

$$v_1(u_1) = 1.2(1 - u_1), \quad u_{1,0}(x) = \sin^2\left(\frac{\pi x}{2}\right), \quad (4.12)$$

$$v_2(u_2) = (1 - u_2), \quad u_{2,0}(x) = \sin^2\left(\frac{\pi x}{2}\right), \quad (4.13)$$

where we can see the results of this simulation in Figure 1. What we see here is that the density in the two lanes tends to flatten out a bit, while the difference in velocity in the two lanes approaches zero.

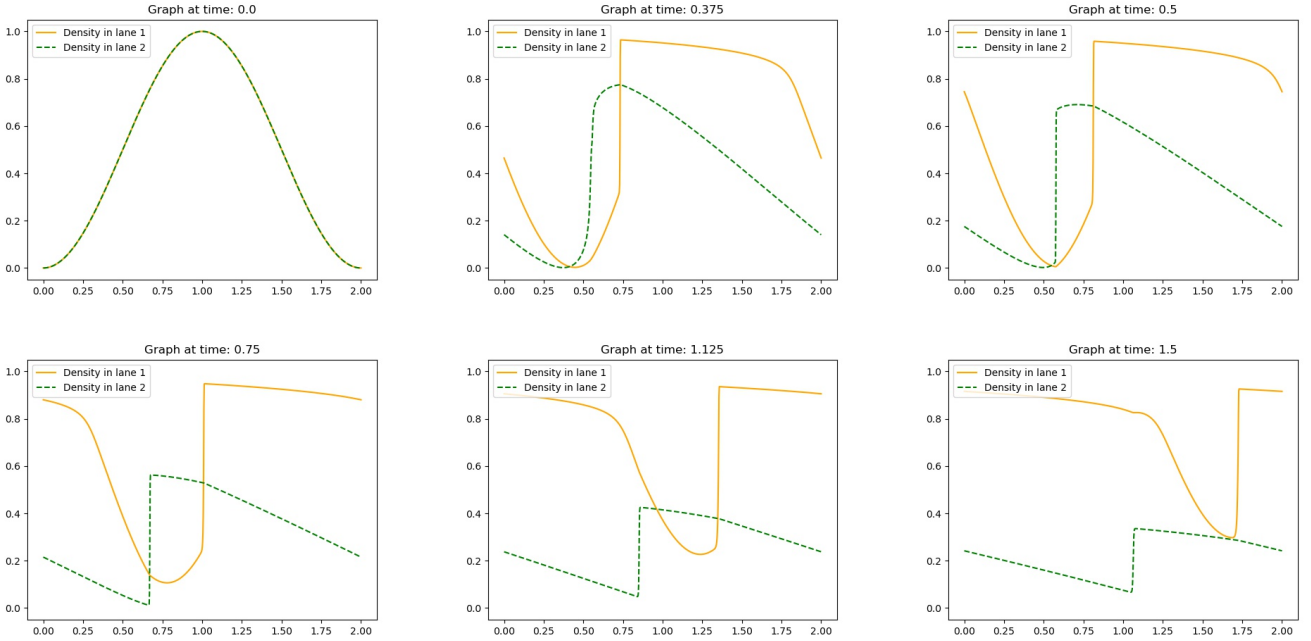


Figure 2: Results from simulations with lane configurations (4.14). The simulations were done using roads of length $l = 2$.

We can also test for two very different velocity functions in the two lanes. Which is a situation we might expect if one lane is either a lot wider or smoother to drive on, allowing greater speeds. We can also expect such a situation if one lane is typically occupied by daredevil drivers. In this simulation, we look at the velocity functions

$$v_1(u) = (1 - u), \quad v_2(u) = 1.2(1 - u^{29}). \quad (4.14)$$

Which from a model perspective implies that lane two has a lot of daredevil drivers, while lane one is much safer to drive in. We use the same initial conditions as the previous simulation. The results of this simulation can be found in Figure 2.

Comparing the two simulations presented so far, we see that despite having changed the velocity function quite a lot, the simulation does show somewhat similar results. We again see the trend that the density of traffic in the two lanes seems to even out and that the difference in velocity between the two lanes appears to have decreased overall.

We finish this section by presenting the results from one last simulation. This time we present the results from a simulation with a very different configuration of the velocity functions and initial conditions of the lanes. We have now used the setup

$$v_1(u_1) = 1.2(1 - u^3), \quad u_1(x, 0) = \sin^2\left(\frac{\pi x}{2} + \pi\right), \quad (4.15)$$

$$v_2(u_2) = (1 - u), \quad u_2(x, 0) = 0.2 + 0.45H_1(x). \quad (4.16)$$

The results of this simulation are presented in Figure 3. Again we see that certain trends repeat from the last few simulations, these being that the densities tend to become more even across the lanes and that the difference in velocity between the lanes seems to decrease.

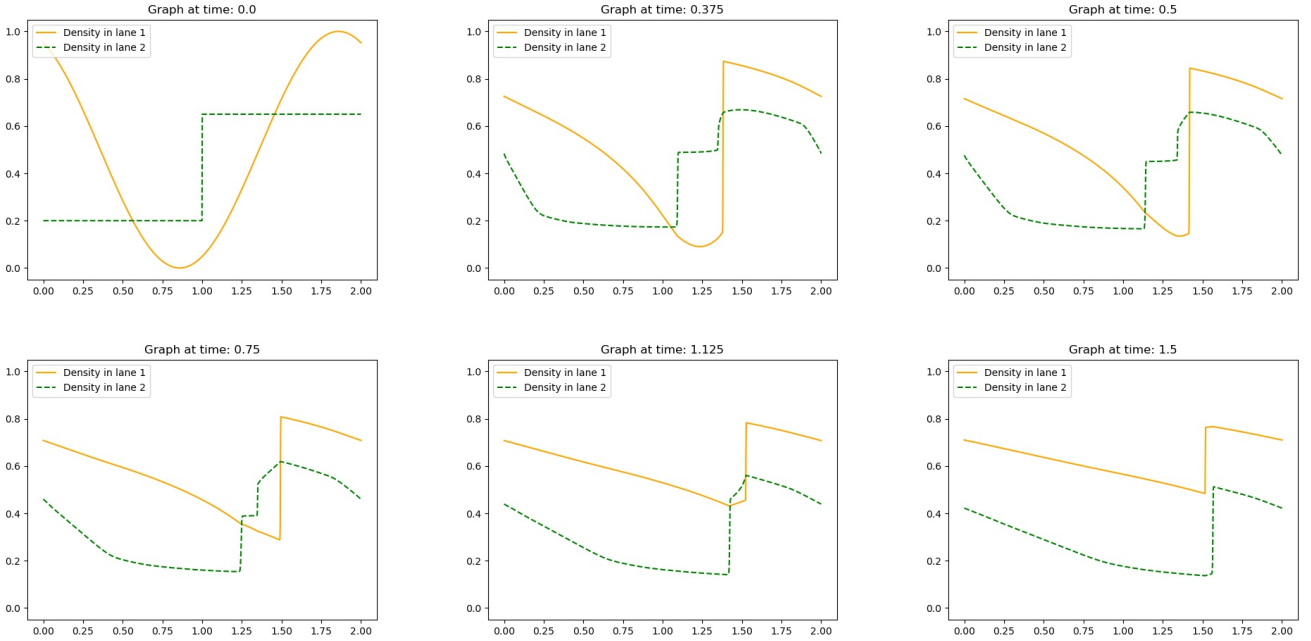


Figure 3: Results from simulations with lane configurations (4.15). The simulations were done using roads of length $l = 2$.

4.2.2 Difference in velocity across lanes

The results from the previous section are also in line with many other similar experiments that have been performed. Thus we are led to define the functional

$$\mathcal{F}(u(\cdot, t)) = \int_{\mathbb{R}} |u_2(x, t) - u_1(x, t)| dx. \quad (4.17)$$

We note here that we have chosen to define \mathcal{F} by integrating over the entire real line. Thus we are led to require u to be such that $|u_2(\cdot, t) - u_1(\cdot, t)|$ is integrable for all t . Another alternative to this requirement is of course to define \mathcal{F} by integrating over some bounded interval on \mathbb{R} instead of the entire real line.

Based on our simulations so far we are tempted to make the proposition that given u which solves (4.1) then $\mathcal{F}(u(\cdot, t))$ will decrease to some lower limit when t grows very large. However, we will need to do some further investigations into this before any conclusions can be made. Especially since any such behaviour may stem from boundary effects.

We might then ask what this lower limit should be. Before we attack these questions with some analytical methods, we study \mathcal{F} using simulations. Noting that for the numerical simulation of \mathcal{F} with periodic boundary conditions we get

$$\mathcal{F}(u^{\Delta t}(\cdot, t)) = \mathcal{F}_n(u^{\Delta t}) = \sum_{j=0}^{J-1} |v_2(u_2^{j,n}) - v_1(u_1^{j,n})| \Delta x, \quad \text{for } t \in [t^n, t^{n+1}), \quad (4.18)$$

where we have $J\Delta x = x_J = l$.

In Figure 4 we present four plots of the evolution in time of \mathcal{F} . The first three are of the lane configurations we used for the simulations already shown, and the fourth graph shows the

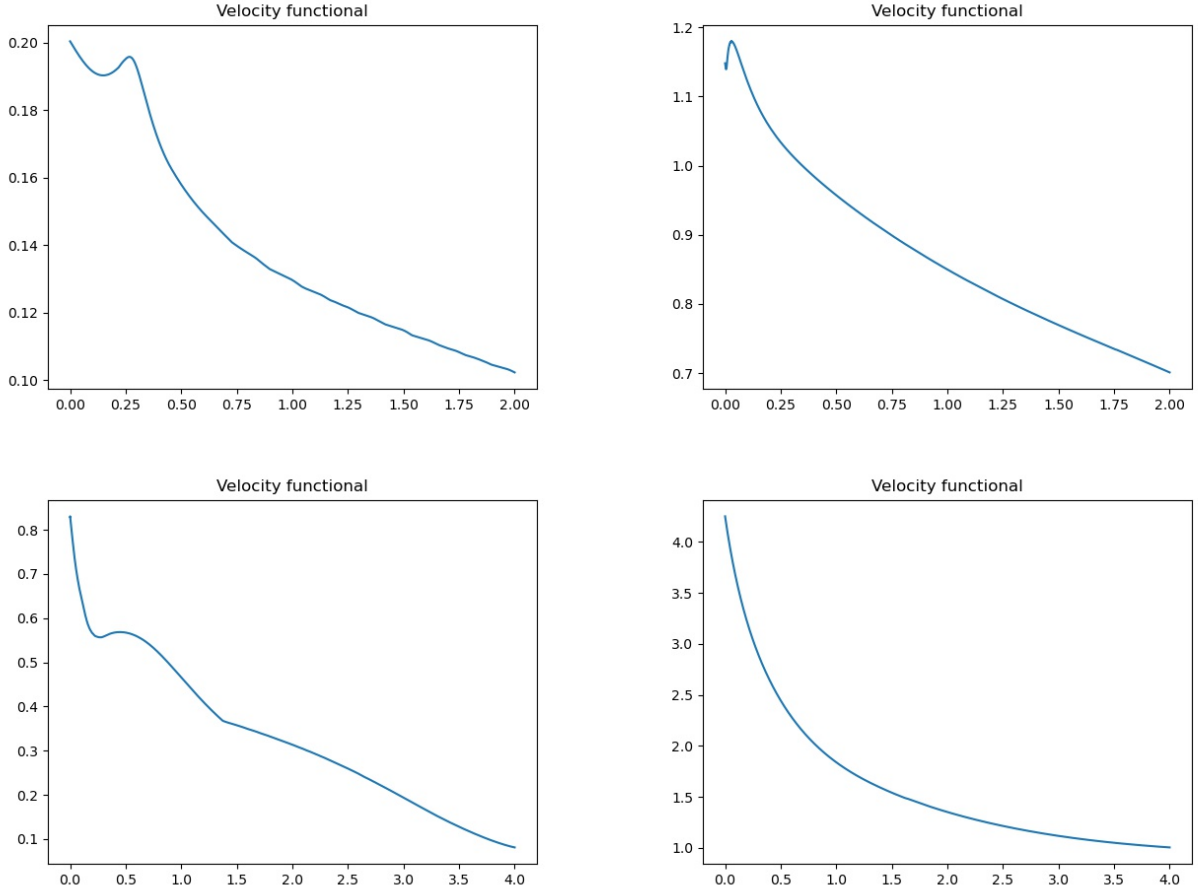


Figure 4: The evolution in time of \mathcal{F} . The top left is for (4.12), the top right is for (4.14), the bottom left is from (4.15), and the bottom right is from (4.19).

evolution in time of \mathcal{F} for the lane configuration

$$v_1(u_1) = 3.0(1 - u), \quad u_1(x, 0) = 0.2 \sin^2\left(\frac{\pi x}{2}\right), \quad (4.19)$$

$$v_2(u_2) = (1 - u), \quad u_2(x, 0) = 0.2 + 0.45H_1(x). \quad (4.20)$$

The main things to note with this last configuration is that there is a great difference in top speeds and that the total number of cars is quite low. We see here that the three first graphs all show \mathcal{F} going towards zero, but the final graph appears to stop and flatten out before it gets to close too zero. It is also worth noting that across all these simulations we see that only the last one appears to be monotonously decreasing, while all the other graphs show at least one increasing section.

We might then wonder what happens to cause the increasing sections and if these sections always will go over to a decreasing section. In the pursuit of a better understanding of how \mathcal{F} changes in time it seems reasonable to once again apply operator splitting in order to study how each operator changes \mathcal{F} . We can study this by looking at

$$\mathcal{H}_n = \frac{\mathcal{F}(u^{n+1}) - \mathcal{F}(u^{n+\frac{1}{2}})}{\Delta t}, \quad \mathcal{G}_n = \frac{\mathcal{F}(u^{n+\frac{1}{2}}) - \mathcal{F}(u^n)}{\Delta t}. \quad (4.21)$$

Where \mathcal{G}_n gives how much the flux step changes the value of \mathcal{F} at the n'th step in time, and \mathcal{H}_n is similar but for the source step.

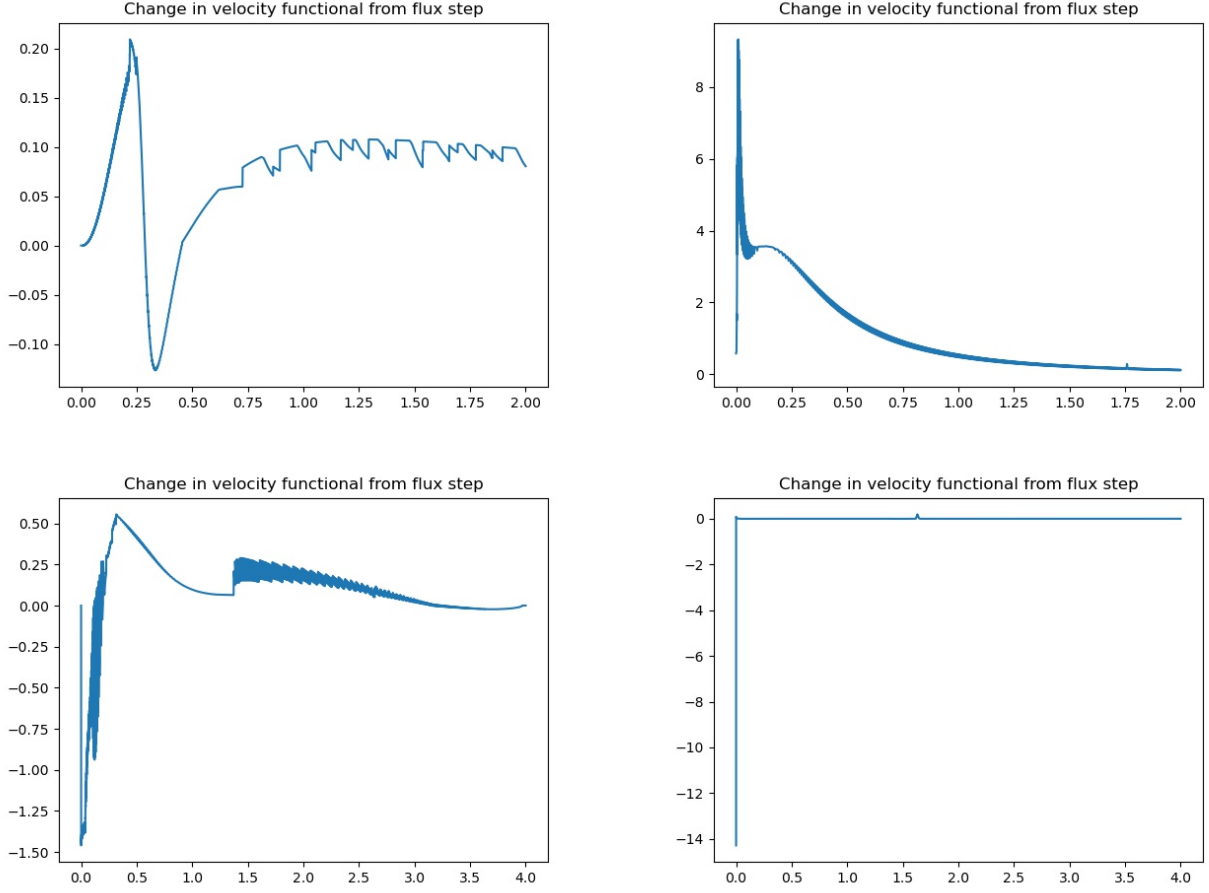


Figure 5: The change in \mathcal{F} across the flux steps. The top left is for (4.12), the top right is for (4.14), the bottom left is from (4.15), and the bottom right is from (4.19).

For the source step, it is rather simple to show that this will always reduce \mathcal{F} . We give a short argument for this fact here. We first focus in on a single j , by the mean value theorem, there exists constants $\zeta_i^{j,n+\frac{1}{2}}$ such that we can do the expansion

$$\begin{aligned}
v_2(u_2^{j,n+1}) - v_1(u_1^{j,n+1}) &= (v_2(u_2^{j,n+\frac{1}{2}}) + v_2'(\zeta_2^{j,n+\frac{1}{2}})\Delta t S(u_1^{j,n+\frac{1}{2}}, u_2^{j,n+\frac{1}{2}})) \\
&\quad - (v_1(u_1^{j,n+\frac{1}{2}}) - v_1'(\zeta_1^{j,n+\frac{1}{2}})\Delta t S(u_1^{j,n+\frac{1}{2}}, u_2^{j,n+\frac{1}{2}})) \\
&= v_2(u_2^{j,n+\frac{1}{2}}) - v_1(u_1^{j,n+\frac{1}{2}}) \\
&\quad + (v_1'(\zeta_1^{j,n+\frac{1}{2}}) + v_2'(\zeta_2^{j,n+\frac{1}{2}}))\Delta t S(u_1^{j,n+\frac{1}{2}}, u_2^{j,n+\frac{1}{2}}).
\end{aligned}$$

We note here that we have

$$\begin{aligned}
&\left| (v_1'(\zeta_1^{j,n+\frac{1}{2}}) + v_2'(\zeta_2^{j,n+\frac{1}{2}}))\Delta t S(u_1^{j,n+\frac{1}{2}}, u_2^{j,n+\frac{1}{2}}) \right| \\
&\leq \left| \max_{s_1, s_2} (v_1'(s_1) + v_2'(s_2))\Delta t (v_2(u_2^{j,n+\frac{1}{2}}) - v_1(u_1^{j,n+\frac{1}{2}})) \right|.
\end{aligned}$$

We see then that if we require

$$\left| \max_{s_1, s_2} (v_1'(s_1) + v_2'(s_2))\Delta t \right| \leq 1, \tag{4.22}$$

we will get $\text{sgn}(v_2(u_2^{j,n+1}) - v_1(u_1^{j,n+1})) = \text{sgn}(v_2(u_2^{j,n+\frac{1}{2}}) - v_1(u_1^{j,n+\frac{1}{2}}))$. Thus, if we assume Δt satisfies (4.22), we get

$$\begin{aligned}\mathcal{H}_n &= \sum_j \left(\frac{\text{sgn}(v_2(u_2^{j,n+\frac{1}{2}}) - v_1(u_1^{j,n+\frac{1}{2}})) \left(v_2(u_2^{j,n+1}) - v_1(u_1^{j,n+1}) - v_2(u_2^{j,n+\frac{1}{2}}) - v_1(u_1^{j,n+\frac{1}{2}}) \right)}{\Delta t} \right) \\ &= \sum_j \frac{1}{\Delta t} \text{sgn}(v_2(u_2^{j,n+\frac{1}{2}}) - v_1(u_1^{j,n+\frac{1}{2}})) \Delta t (v_1'(\zeta_1^{j,n+\frac{1}{2}}) + v_2'(\zeta_2^{j,n+\frac{1}{2}})) \\ &= \sum_j (v_1'(\zeta_1^{j,n+\frac{1}{2}}) + v_2'(\zeta_2^{j,n+\frac{1}{2}})) \left| S(u_1^{j,n+\frac{1}{2}}, u_2^{j,n+\frac{1}{2}}) \right|.\end{aligned}$$

Since the derivative of the velocity functions are required to be negative we can conclude then that $\mathcal{H}_n \leq 0$. We note also that equality can only happen when either the velocity is equal in both lanes, meaning $\mathcal{F} = 0$, or when the density in the slowest lane is equal to zero. This second case is then what happens in (4.19). However, we see that the behaviour of \mathcal{H}_n is easily understood, and will clearly hold to the limit when Δt goes to zero.

The flux step is more interesting in this setting, as this is will be the only source of increase in \mathcal{F} . We again show the results of simulations for the earlier lane configurations, see Figure 5. We see here that \mathcal{G}_n can be both positive and negative.

The graphs in Figure 5 are not very helpful on their own. In order to see what is going on "under the hood" of \mathcal{F} , we will need to also study how the densities of vehicles in each lane are distributed at the times where \mathcal{G}_n is the most positive. This was done through use of animations. In short, what was found when comparing these animations to 5 is that \mathcal{G}_n becomes very negative when each lane has a shock, but the shocks in the two lanes are travelling at different speeds. We try to illustrate this phenomenon by looking at a simple example. We study the evolution of \mathcal{F} under the equation

$$\begin{aligned}\partial_t u_1 + \partial_x(u_1(1 - u_1)) &= 0, & u_1(x, 0) &= 0.4\mathbf{H}_0(x), \\ \partial_t u_2 + \partial_x(u_2 2.0(1 - u_2)) &= 0, & u_2(x, 0) &= 0.5 + 0.2\mathbf{H}_0(x),\end{aligned}$$

in order to better present this phenomenon.

This is of course equivalent to using a linear velocity function in both lanes, with a double speed limit in the second lane, with no lane switching. Application of the standard Rankine-Hugoniot condition to each of these gives us the solutions

$$\begin{aligned}u_1(x, t) &= 0.4\mathbf{H}_{0.6t}(x), & u_2(x, t) &= 0.5 + 0.2\mathbf{H}_{-0.8t}(x), \\ v_1(u_1(x, t)) &= 1 - 0.4\mathbf{H}_{0.6t}(x), & v_2(u_2(x, t)) &= 2 - 1.6\mathbf{H}_{-0.8t}(x),\end{aligned}$$

Thus we can easily calculate the value of \mathcal{F} to be

$$\mathcal{F}(u(\cdot, t)) = 0.4(0.6 + 0.8)t = 0.56t.$$

Thus we get an increase in \mathcal{F} due to the different velocity of the fronts. However, this is before we include the effect of the source term. In the next section we then aim to do a closer study of the more complete picture we get from including the effect of the source term again.

4.2.3 Riemann problem simulations

The result we got from looking at (4.24), was very interesting, and inspires us to look closer at some simulations of Riemann problems for (4.1). We recall that a Riemann problem is a

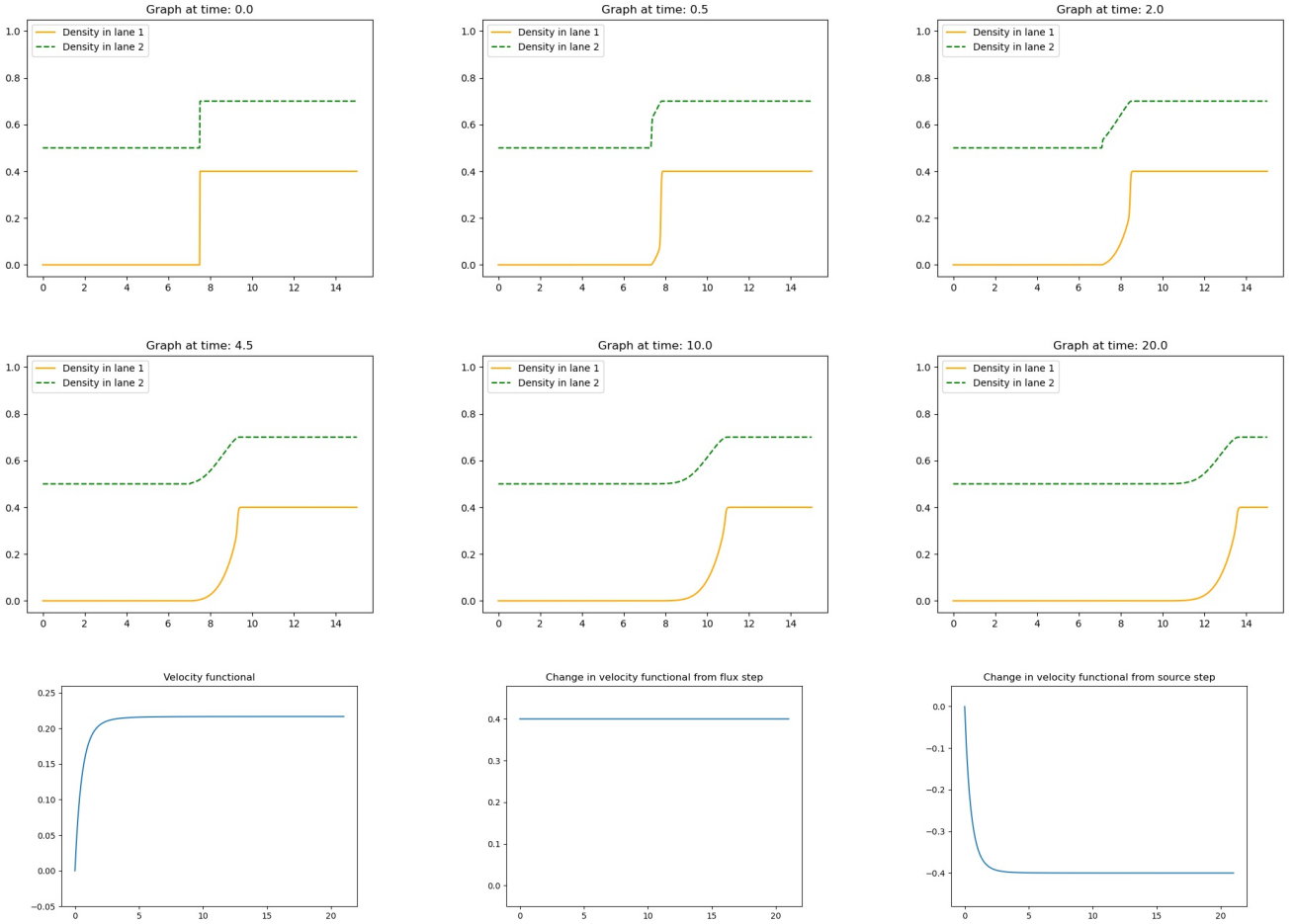


Figure 6: Simulation results with the lane configuration from (4.24), but with the source added back in. The two top rows show the result of the simulation, while the last row shows first a plot of the \mathcal{F} , then a plot of \mathcal{G} , and finally a plot of \mathcal{H} .

problem with initial conditions of the form

$$u_0(x) = u_l + (u_r - u_l)\mathbf{H}_0(x) = \begin{cases} u_l, & x \leq 0, \\ u_r, & x > 0. \end{cases} \quad (4.23)$$

Due to the constant values when going far out along the x-axis we can ignore the boundary conditions and simply run simulations with no effect from the boundary. We can then start by looking at what happens to (4.24) after we reintroduce the source term. This means simulating with the lane configuration

$$v_1(u_1) = 1 - u_1, \quad u_{1,0}(x) = 0.6\mathbf{H}_0(x), \quad (4.24)$$

$$v_2(u_2) = 2(1 - u_2), \quad u_{2,0}(x) = 0.5 + 0.3\mathbf{H}_0(x). \quad (4.25)$$

The results of this simulation can be seen in Figure 6.

Looking closely at this simulation we seem to reach a point where we reach a solution, and after this the evolution in time is only a translation. We see that both the velocity functional and the change in the velocity functional from the flux step flattens out. We seem to have reached a point of balance between the effect from the flux step and the effect from the source step. Thus this simulation appears to give a clear example where \mathcal{F} will not end up at zero.

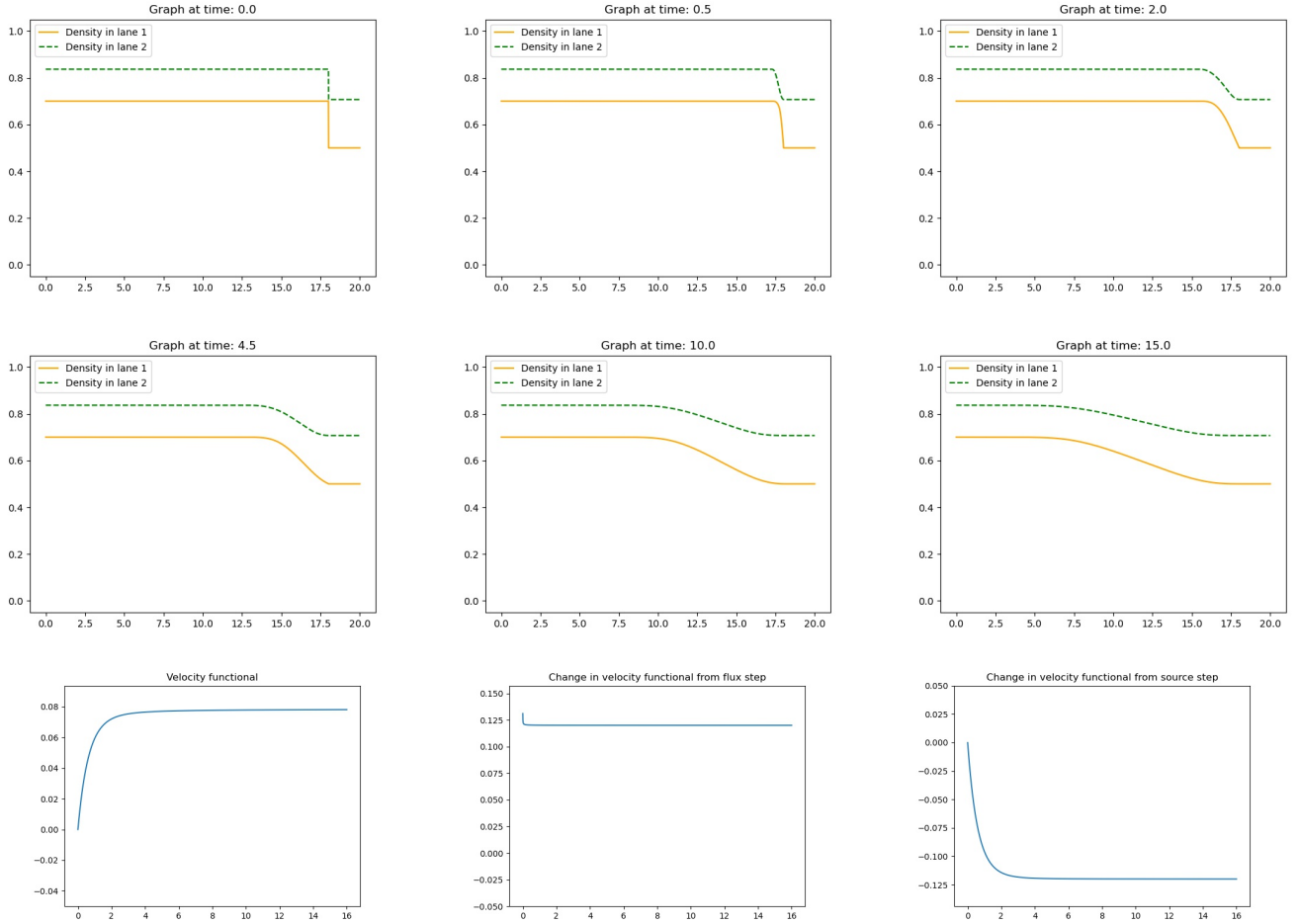


Figure 7: Simulation results with the lane configuration from (4.26). The two top rows show the result of the simulation, while the last row shows first a plot of the \mathcal{F} , then a plot of \mathcal{G} , and finally a plot of \mathcal{H} .

In this first example, we had increasing initial conditions, which gives a shock from the flux operator. It can be interesting to check out the simulation for initial conditions which give two different rarefaction waves instead of the travelling shocks. We then choose the lane configuration

$$v_1(u_1) = 1 - u_1, \quad u_{1,0}(x) = 0.7 - 0.2H_0(x), \quad (4.26)$$

$$v_2(u_2) = 1 - u_2^2, \quad u_{2,0}(x) = \sqrt{0.7} - (\sqrt{0.7} - \sqrt{0.5})H_0(x). \quad (4.27)$$

Again we have a lane configuration where $\mathcal{F}(u_0) = 0$. We also switched up the velocity function a bit, which might also give us some interesting behaviour. The results from this simulation are displayed in Figure 7. Upon closer inspection of these simulations, we see that the evolution of \mathcal{F} follows a similar trend as the trend seen in Figure 6. We start with \mathcal{G} taking some value greater than zero, and staying almost constant. While \mathcal{H} starts at zero and grows until it is equal to $-\mathcal{G}$. After this point is reached \mathcal{F} appears to stay at a constant value. Looking at the simulation itself we see that we have two rarefaction waves moving to the left, giving a solution in which the steepness of the curve appears to become ever lesser the longer we go.

Thus far we have then seen two rather interesting problems where we start with \mathcal{F} equal to zero, and then \mathcal{F} appears to "settle" at some value which is greater than zero. It can then be

interesting to study a different configuration where the initial conditions of the two lanes are a bit less similar. We then chose to run simulations with the lane configuration

$$v_1(u_1) = 1 - u_1^3, \quad u_{1,0}(x) = 0.4^{\frac{1}{3}} + (0.8^{\frac{1}{3}} - 0.4^{\frac{1}{3}})H_{18}(x), \quad (4.28)$$

$$v_2(u_2) = 1 - u_2^2, \quad u_{2,0}(x) = 0.4^{\frac{1}{2}} + (0.2^{\frac{1}{2}} - 0.4^{\frac{1}{2}})H_{15}(x). \quad (4.29)$$

The results from this simulation are shown in Figure 8. With these results, we see an asymptotic

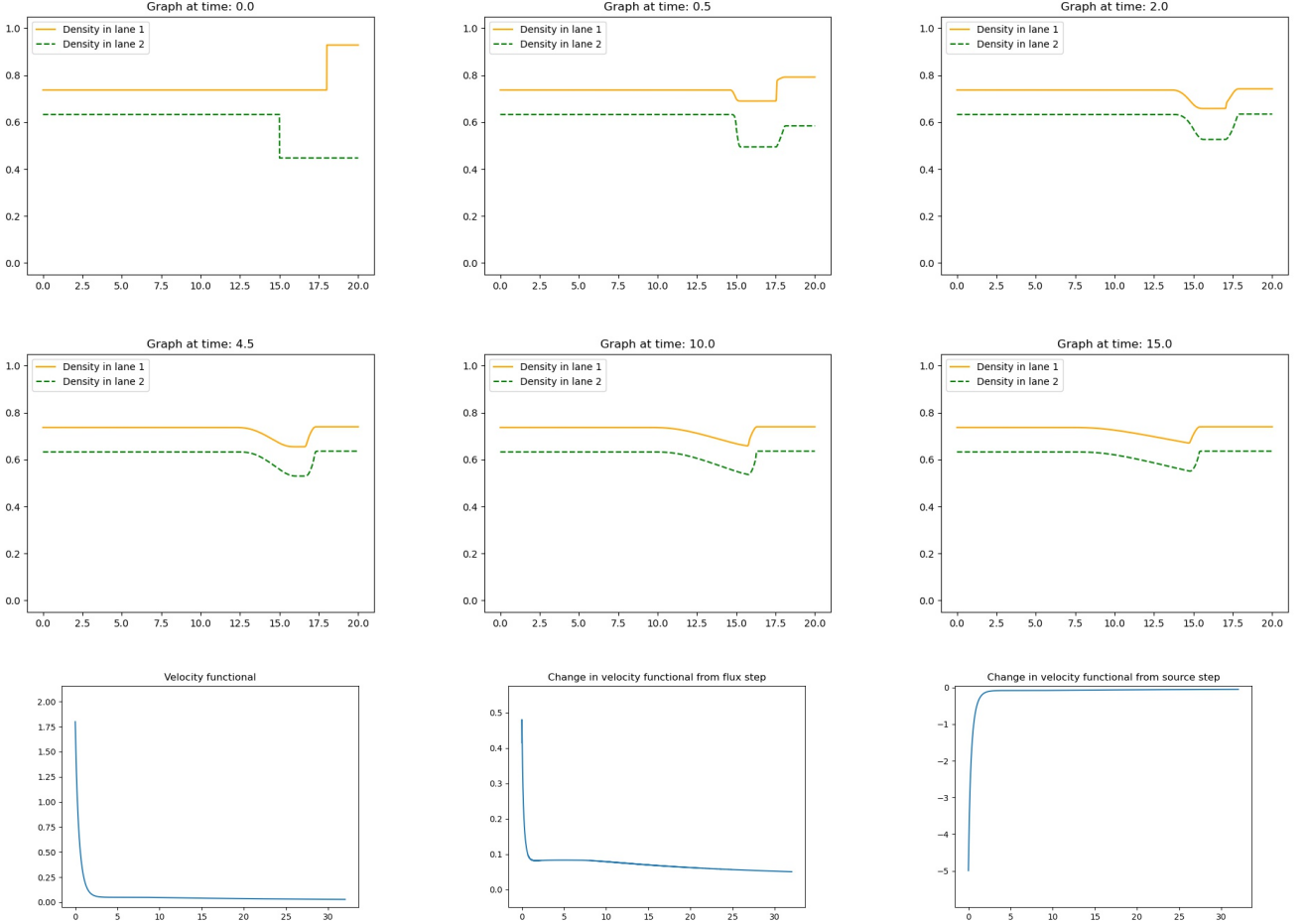


Figure 8: Simulation results with the lane configuration from (4.28), but with the source added back in. The two top rows show the result of the simulation, while the last row shows first a plot of the \mathcal{F} , then a plot of \mathcal{G} , and finally a plot of \mathcal{H} .

behaviour where \mathcal{F} does appear to get close to zero. Though it is hard to say for sure if there is some lower bound similar to what we had with (4.24), or if it will go to zero in the limit. This is hard to say because in the simulations done, it does not get within machine error range of zero, but still appears to be decreasing. Looking at the behaviour of the density in the two lanes, we see a tendency for the graphs to flatten out. Similarly to the simulations we did with periodic boundary conditions.

4.2.4 Model interpretation

We finish the section on our simulations with a short interpretation of the results in terms of traffic flow. The main result we seem to have obtained is that generally, the overall difference

in velocity between the two lanes seems to decrease. This is as one might expect, as the model is built upon the assumption that cars will change lanes when the vehicles in the neighbouring lane move faster.

The other result we saw was that shocks from two lanes moving in different directions can lead to an increase in the difference in velocity across the lanes. This can be interpreted as what might happen if one lane has some congestion while the other moves along more smoothly. Then the congestion will expand backwards, which will increase the length of road where there is a difference in traffic flow. Again we have then a result that seems to be as one might expect from the traffic flow point of view.

5 Analytical results regarding multilane traffic flow

We now finish with a section where we aim to prove some of the proposed asymptotic behaviour of (4.1).

We will start these investigations by looking at some properties of (4.1), which will not be directly related to the evolution of \mathcal{F} . Then we will move on to look closer at the evolution of \mathcal{F} , first by studying \mathcal{F} under smooth solutions of (4.1). Then we will establish how we can apply operator splitting for studying the evolution of \mathcal{F} , before we use this to study \mathcal{F} given some special cases. This will finish by looking at a class of cases where \mathcal{F} will not go to zero.

5.1 General properties of the two lane system

Before we start looking at the evolution of \mathcal{F} , we look at some general properties of solutions to (4.1). First we quickly show this nice little property relating to monotone initial conditions.

Lemma 5.1. *Suppose $u_{1,0}$, and $u_{2,0}$ to both be increasing, or both be decreasing. Then let u be a solution to (4.1) with $u_{i,0}$ as initial conditions in lane i . Then for any given time, t , $u_i(\cdot, t)$ will be increasing/decreasing.*

Proof. Let $\{u_i^{j,n}\}$ be computed by a consistent, conservative and monotone method as in (3.5). We note that the flux step is immediately monotonicity preserving due to 2.4. Thus we need only check that the source step will not change that. This can be done quite simply by looking at the partial derivatives of the source step. To do this we first need to find the derivatives of the source function.

$$\partial_u S(u, w) = (v_2(w) - v_1(u))^+ - v_1'(u) \begin{cases} u, & v_2(w) \geq v_1(u), \\ v, & v_2(w) < v_1(u), \end{cases}$$

$$\partial_w S(u, w) = -(v_2(w) - v_1(u))^- + v_2'(w) \begin{cases} u, & v_2(w) \geq v_1(u), \\ v, & v_2(w) < v_1(u), \end{cases}$$

Note in particular here that $\partial_u S(u, w) \leq 0$, and $\partial_w S(u, w) \geq 0$. With this established, we look at the derivatives of the source step in lane one.

$$\frac{\partial u_1^{j,n+1}}{\partial u_1^{j,n+\frac{1}{2}}} = 1 - \Delta t \left(\frac{\partial}{\partial u_1^{j,n+\frac{1}{2}}} S(u_1^{j,n+\frac{1}{2}}, u_2^{j,n+\frac{1}{2}}) \right) \geq 1,$$

$$\frac{\partial u_1^{j,n+1}}{\partial u_1^{j,n+\frac{1}{2}}} = \Delta t \left(\frac{\partial}{\partial u_1^{j,n+\frac{1}{2}}} S(u_1^{j,n+\frac{1}{2}}, u_2^{j,n+\frac{1}{2}}) \right) \geq 0.$$

This allows us then to easily conclude that if $u_i^{j,n+\frac{1}{2}} \leq u_i^{j+1,n+\frac{1}{2}}$ for both lanes. Then it follows that $u_1^{j,n+1} \leq u_1^{j+1,n+1}$. We can do a very similar argument for lane two. Which will allow us to conclude that the source step will preserve the monotonicity. We see thus that both the source step and the flux step will preserve monotonicity. Since this monotonicity is not dependent on Δt , we can conclude that it still holds after taking the limit of $\Delta t \rightarrow 0$. \square

This next property sounds more complicated, but it really stems from simple considerations related to the stability of the source step. We note also that any system with monotone initial conditions will also be of bounded total variation, so this next theorem will also apply in those situations.

Lemma 5.2. *Suppose $u(x, t)$ solves (4.1) with initial conditions $u_0(x) = \{u_{1,0}(x), u_{2,0}(x)\}$. Suppose $u_{i,0}$ to be of bounded total variation for each lane i , implying that for each lane i , there exists limits,*

$$0 \leq u_{0,i}^{r/l} = \lim_{x \rightarrow \pm\infty} u_{i,0}(x) \leq 1.$$

Then for any t , $u_i(\cdot, t)$ will be of bounded variation, with $0 \leq u_i^{r/l}(t) = \lim_{x \rightarrow \pm\infty} u_i(x, t) \leq 1$. Furthermore, we have that $\left| S(u_2^{r/l}(t), u_1^{r/l}(t)) \right|$ goes to zero as $t \rightarrow \infty$.

Proof. Let $\{u_i^{j,n}\}$ be computed by a consistent, conservative and monotone method as in (3.5), for solving the traffic problem, (4.1). Making only the change that the source step is calculated analytically instead of by use of the forward Euler method. We denote $u_{i,l/r}^n = \lim_{j \rightarrow \pm\infty} u_i^{j,n}$. We will first show, that the flux step will not cause $u_{i,l/r}^n$ to change. We look at the limit $\lim_{j \rightarrow -\infty} u_i^{j,n+\frac{1}{2}}$, by noting the following

$$\begin{aligned} \left| u_{i,l} - u_i^{j,n+\frac{1}{2}} \right| &= \left| u_{i,l} - u_i^{j,n} + \lambda \left| F_i^{j+\frac{1}{2},n} - F_i^{j-\frac{1}{2},n} \right| \right| \\ &\leq \left| u_{i,l} - u_i^{j,n} \right| + \lambda \left| F_i^{j+\frac{1}{2},n} - F_i^{j-\frac{1}{2},n} \right| \\ &\leq \left| u_{i,l} - u_i^{j,n} \right| + \|F_i\|_{Lip} \lambda \left(\left| u_i^{j-p,n} - u_i^{j-p-1,n} \right| + \dots + \left| u_i^{j+q,n} - u_i^{j+q-1,n} \right| \right). \end{aligned}$$

Note then that letting $j \rightarrow -\infty$ every term in the final inequality will go to zero, thus $u_{i,l}^{n+\frac{1}{2}} = u_{i,l}^n$. We note that essentially the same proof will hold for $u_{i,r}^n$.

Next we do the source step. We start by noting that due to the continuity of S , we can move the limit of $j \rightarrow \pm\infty$ to the outside. So really we need only that $S(u_{1,l/r}^n, u_{2,l/r}^n)$ goes to zero. Since we are using the exact solution for the source step, and the flux step doesn't change the value of $u_{i,l}^n$, we need only show that under the evolution of the ODE

$$\dot{u}_i = (-1)^i S(u_1, u_2), \quad u_i(0) = u_{0,i}^l,$$

the value of $S(u_1, u_2)$ goes to zero. This is most easily seen by utilizing standard stability theory, noting that we have a stable point at $S(u_1, u_2) = 0$. See Section 4 from [22] for a more detailed proof of this last statement. \square

We use this property to argue that for initial conditions of bounded variation, it is only of interest to study initial conditions with

$$\lim_{x \rightarrow \pm\infty} v_2(u_{2,0}) = \lim_{x \rightarrow \pm\infty} v_1(u_{1,0}(x)). \quad (5.1)$$

As the above lemma gives that for any initial condition with bounded variation will asymptotically approach this exact condition. We note also that (5.1) is actually a requirement for $\mathcal{F}(\cdot, t) < \infty$ to hold.

5.2 Smooth case

We start our exploration of how $\mathcal{F}(u(\cdot, t))$, develops in time by looking at what might happen in the case where we assume $u = \{u_1, u_2\}$ to be a smooth solution to (4.1).

We start by looking at the derivative in time of $\mathcal{F}(u(\cdot, t))$, which initially gives:

$$\begin{aligned}
\frac{d}{dt} \int_{\mathbb{R}} |v_2(u_2) - v_1(u_1)| dx &= \int_{\mathbb{R}} \operatorname{sgn}(v_2 - v_1) (v_2'(u_2) \partial_t u_2 - v_1'(u_1) \partial_t u_1) dx \\
&= \int_{\mathbb{R}} \operatorname{sgn}(v_2 - v_1) (v_2'(u_2) (S(u_1, u_2) - \partial_x(u_2 v_2(u_2))) - v_1'(u_1) (-S(u_1, u_2) - \partial_x(u_1 v_1(u_1)))) dx \\
&= \int_{\mathbb{R}} \operatorname{sgn}(v_2 - v_1) (v_2'(u_2) + v_1'(u_1)) S(u_1, u_2) dx \\
&+ \int_{\mathbb{R}} \operatorname{sgn}(v_2 - v_1) (v_1'(u_1) \partial_x f_1(u_1) - v_2'(u_2) \partial_x f_2(u_2)) dx.
\end{aligned}$$

We recognize here that the first term is the effect from the source term, while the second term is the effect from the conservation law. This leads us to define

$$\mathcal{H} = \int_{\mathbb{R}} \operatorname{sgn}(v_2 - v_1) (v_2'(u_2) + v_1'(u_1)) S(u_1, u_2) dx, \quad (5.2)$$

and

$$\mathcal{G} = \int_{\mathbb{R}} \operatorname{sgn}(v_2 - v_1) (v_1'(u_1) \partial_x f_1(u_1) - v_2'(u_2) \partial_x f_2(u_2)) dx. \quad (5.3)$$

These are then defined in a similar manner to the definitions in (4.21), in the sense that \mathcal{G} represents the change to \mathcal{F} from the hyperbolic conservation law, while \mathcal{H} represents the change to \mathcal{F} from the source function. We can then simply study each of these terms individually, starting with \mathcal{H} .

We note first that by assumption we have $v_i'(u_i) < 0$ for both lanes. Thus we can conclude that $\mathcal{H} \leq 0$, with equality only if for almost every x one of the following three conditions holds:

- (i) $v_1(u_1(x, t)) = v_2(u_2(x, t))$.
- (ii) $u_2(x, t) = 0$, and we have $v_1(u_1(x, t)) > v_2(u_2(x, t))$.
- (iii) $u_1(x, t) = 0$, and we have $v_1(u_1(x, t)) \leq v_2(u_2(x, t))$.

Thus we can conclude that the effect from the source term on \mathcal{F} will be to decrease it towards some lower bound. Furthermore, this lower bound will depend on the difference in speed limit for the two lanes, and the density of traffic of the two lanes combined. From the perspective of traffic modelling, this is equivalent to either the velocity in both lanes being equal or one lane being empty while there is still no possible gain in speed from switching lanes. It is worth noting here that the second of these outcomes can only happen if one lane has a greater speed limit than the other.

We now move on to study \mathcal{G} closer. We note that if we define

$$\gamma_i'(u_i) = v_i'(u_i) f_i'(u_i). \quad (5.4)$$

We get

$$\mathcal{G}(u) = \int_{\mathbb{R}} \operatorname{sgn}(v_2 - v_1) \partial_x [\gamma_1(u_1) - \gamma_2(u_2)] dx.$$

From the perspective of traffic modelling, $\partial_x \gamma_i(u_i(x, t))$ will then model how the velocity of vehicles changes in lane i at coordinate (x, t) , when ignoring the effect from vehicles changing lane. Here we assume that $\operatorname{sgn}(v_2 - v_1)$ changes value at a finite number of points, $\{x_1, x_2, \dots, x_N\}$.

We assume also that $v_2 - v_1 = 0$ in $(-\infty, x_1]$, in $[x_N, \infty)$, and in $[x_j, x_{j+1}]$ for every $j \in J$ where J is some finite index set.

$$\begin{aligned} \mathcal{G}(u) &= \sum_{k \notin J} \operatorname{sgn}(\delta_v(x \in (x_k, x_{k+1}))) \int_{x_k}^{x_{k+1}} \partial_x [\gamma_1(u_1) - \gamma_2(u_2)] dx \\ &= \sum_{k \notin J} \operatorname{sgn}(\delta_v(x \in (x_k, x_{k+1}))) ([\gamma_1(u_1(x_{k+1})) - \gamma_2(u_2(x_{k+1}))]) \\ &\quad - \sum_{k \notin J} \operatorname{sgn}(\delta_v(x \in (x_k, x_{k+1}))) ([\gamma_1(u_1(x_k)) - \gamma_2(u_2(x_k))]). \end{aligned}$$

We can then see that only the value of u at the points $\{x_1, \dots, x_N\}$ will be needed to determine the value of $\mathcal{G}(u)$. For a Greenshield type velocity function, $v_i(u) = c_i(1 - u^{n_i})$ we can easily calculate γ_i explicitly to be

$$\gamma_i(u_i) = c_i^2 u_i^{n_i} \left(\frac{1 + n_i}{2} u_i^{n_i} - 1 \right).$$

As we can see, we can easily construct functions where $v_1(u_1) = v_2(u_2)$, but $\gamma_1(u_1) \neq \gamma_2(u_2)$. What we can then see is that even in the case of relatively simple velocity functions in each lane, we still end up with complicated functions, γ_i . To work around these difficulties stemming from the effect of the hyperbolic conservation law, we will need to focus on simpler special cases, where we can come with conclusions on the asymptotic behaviour of \mathcal{F} .

A remark that is worth making here is that in the case where we have the same velocity function in both lanes, i.e. $v_1(w) = v_2(w)$ for all w . We will have $\gamma_1(w) = \gamma_2(w)$, and $u_1 = u_2$ at every point in $\{x_1, \dots, x_N\}$. Thus we get $\mathcal{G}(u) = 0$. This means that in the case where both lanes have the same velocity functions the difference in velocity across the lanes will only change due to the source step.

5.3 Operator splitting

An important tool in showing these properties will be operator splitting, which will allow us to look at how each of the operators affects \mathcal{F} . Thus we would study separately

$$\mathcal{G}_{\Delta t}(w) = \mathcal{F}(W(\Delta t)w) - \mathcal{F}(w), \quad (5.5)$$

and

$$\mathcal{H}_{\Delta t}(w) = \mathcal{F}(R(\Delta t)w) - \mathcal{F}(w). \quad (5.6)$$

Here we can think of $\mathcal{H}_{\Delta t}(u, t)$ as how the source step changes the difference in velocity. Similarly $\mathcal{G}_{\Delta t}(u, t)$ as how much the flux step will change the difference in velocity. We note then that

$$\mathcal{F}(u^{\Delta t}(\cdot, t^n)) = \sum_{k=0}^{n-1} \mathcal{G}_{\Delta t}(u^k) + \mathcal{H}_{\Delta t}(u^{k+\frac{1}{2}}) + \mathcal{F}(u^{\Delta t}(\cdot, 0)).$$

Thus if we can show some general properties independent of Δt for $\mathcal{G}_{\Delta t}$, and $\mathcal{H}_{\Delta t}$ we also get some general property of $\mathcal{F}(u^{\Delta t}(\cdot, t_n))$ again independently of Δt .

Finally we make the claim that $\mathcal{F}(u(\cdot, t)) = \lim_{\Delta t \rightarrow 0} \mathcal{F}(u^{\Delta t}(\cdot, t))$. For the sake of simplicity, we assume that the support in the x-coordinate of $|v_2(u_2^{\Delta t}(x, t^n)) - v_1(u_1^{\Delta t}(x, t^n))|$ can be bounded by the interval $[-M, M]$. Then we have that the constant function $g(x) = (|v_2(0) - v_1(1)| +$

$|v_2(1) - v_1(0)|)(H_{-M} - H_M)$, which will work as a dominating function for the application of Lebesgue dominated convergence theorem. Thus we can indeed conclude that

$$\mathcal{F}(u(\cdot, t)) = \lim_{\Delta t \rightarrow 0} \mathcal{F}(u^{\Delta t}(\cdot, t)). \quad (5.7)$$

The next step is to look for more general properties of the two different step changes in \mathcal{F} .

5.4 Effect from the source step

We start this section by recalling that the source step operator, $R(t)$, is defined as the solution operator to the equation

$$\partial_t u_i = (-1)^i (v_2(u_2) - v_1(u_1)) \begin{cases} u_1, & v_2(u_2) \geq v_1(u_1), \\ u_2, & v_2(u_2) < v_1(u_1). \end{cases} \quad (5.8)$$

We note that for each x this is a simple ODE, to which we can apply standard ODE theory. We take the derivative in time of the difference in velocity at some given x ,

$$\frac{d}{dt} |v_2(u_2) - v_1(u_1)| = \text{sgn}(v_2(u_2) - v_1(u_1)) (v_2'(u_2) + v_1'(u_1)) (v_2(u_2) - v_1(u_1)) S(u_1, u_2).$$

We note that

$$\text{sgn}(v_2 - v_1) S(u_1, u_2) = |v_2(u_2) - v_1(u_1)| \begin{cases} u_2, & v_2(u_2) < v_1(u_1), \\ u_1, & v_2(u_2) \geq v_1(u_1), \end{cases}$$

which means that $\text{sgn}(v_2 - v_1) S(u_1, u_2) \geq 0$. Since v_1, v_2 are both strictly decreasing we can further conclude that $\frac{d}{dt} |v_2(u_2) - v_1(u_1)| \leq 0$, with equality only when $S(u_1, u_2) = 0$, which will only occur for

- $v_2(u_2) = v_1(u_1)$,
- $v_2(u_2) > v_1(u_1)$ and $u_1 = 0$,
- $v_2(u_2) < v_1(u_1)$ and $u_2 = 0$.

Each of these cases will then be a stable equilibrium point for (5.8). We can then use this stability to conclude that $\mathcal{F}(u(\cdot, t))$ will go to some lower bound, which need not be zero under the effect of the source step. For more details on this, we refer to standard stability theory in [21], and section 4 of [22].

Thus we can conclude this section by stating that $\mathcal{H} \leq 0$, with equality only if the requirements from the list above are held.

We note that the final two cases can only happen for cases where the speed limit is different in the two lanes, and the overall traffic density is not too high. From our simulations in the previous section, we note that this is exactly what happens for (4.19), explaining why this did not go to zero. It is worth putting some extra emphasis that this does give an easy method for finding examples where \mathcal{F} will then not go to zero. We need only make the velocity functions radically different, or have very low total density of traffic. These examples are however based on configurations where it is simply not possible for \mathcal{F} to become zero, even with a redistributing of the traffic density. Therefore we would also be interested in a case where it is possible to have $\mathcal{F} = 0$, but the flux step causes this to not happen.

5.5 Equal velocity function in both lanes

We start looking at the special case where we have the same velocity function in both lanes. This is in reality the situation we would expect to most often see out on real world roads. Then we can first apply the Lipschitz continuity of the velocity function to obtain

$$\int |v(u_2) - v(u_1)| dx \leq \|v\|_{Lip} \int |u_2 - u_1| dx.$$

Therefore we start by looking at the last term, and not the actual definition of \mathcal{F} . We apply a similar splitting of operators as described in section 5.1. Due to the L^1 -contractivity of scalar hyperbolic conservation laws we can easily conclude that

$$\int |W(t)u_2 - W(t)u_1| dx \leq \int |u_2 - u_1| dx. \quad (5.9)$$

We next look at the change to $|u_2 - u_1|$ due to the source term. This can be done in a similar way as in the previous section, taking the derivative in time to get

$$\begin{aligned} \frac{d}{dt}|u_2 - u_1| &= \text{sgn}(u_2 - u_1)2S(u_1, u_2) \\ &= 2\text{sgn}(u_2 - u_1)(v(u_2) - v(u_1)) \begin{cases} u_2, & v(u_2) \leq v(u_1), \\ u_1, & v(u_2) > v(u_1), \end{cases} \\ &= -2|v(u_2) - v(u_1)| \begin{cases} u_2, & v(u_2) \leq v(u_1), \\ u_1, & v(u_2) > v(u_1). \end{cases} \end{aligned}$$

Thus we can conclude that $\frac{d}{dt}|u_2 - u_1| \leq 0$ under the effect of the source term, with equality only for $u_1 = u_2$. Thus we can conclude that given initial conditions such that $\mathcal{F}(u_0) \leq 0$, we can conclude that $\mathcal{F}(u(\cdot, t))$ goes to zero asymptotically.

We end this section with some model remarks. Note firstly that in the majority of real world cases, the two lanes will be practically identical. Thus it is fair to assume that many real world multilane roads will have lanes with the same velocity functions in all lanes. Thus we conclude that in most roads where (4.1) is a good approximation of how traffic will evolve, the different lanes will have very similar densities of vehicles, with most vehicles driving at almost the same speed.

5.6 A class of counterexamples

Thus far most of the results we have obtained have given the impression that \mathcal{F} will approach some lower limit, which is decided by the conditions in 5.4. However, if we look back to the simulation results from Section 4.2.3, we see that this simulation indicates a different behaviour. In this final section we look at some counterexamples to show that the complicated behaviour from the source step can in many cases cause \mathcal{F} not to be decreasing at all.

For this entire section we will use linear velocity functions in both lanes, which after potentially scaling the equation gives us velocity functions

$$v_1(u_1) = 1 - u_1, \quad v_2(u_2) = c(1 - u_2). \quad (5.10)$$

We assume also also that $c > 1$, this can always be achieved by simply reordering the indices. For this entire section we will also assume that we have initial conditions of bounded variation, satisfying (5.1).

We study then how \mathcal{F} , changes with the flux step of (4.6). Note then that the unique maximum point of f_i is given for both lanes as $\omega = \frac{1}{2}$. We start out by looking at what happens without the absolute value at a specific grid point. Here we then have

$$\begin{aligned} v_2(u_2^{j,n+\frac{1}{2}}) - v_1(u_1^{j,n+\frac{1}{2}}) &= c(1 - (u_2^{j,n} - \lambda(f_2^{EO}(u_2^{j,n}, u_2^{j+1,n}) - f_2^{EO}(u_2^{j-1,n}, u_2^{j,n})))) \\ &\quad - (1 - (u_1^{j,n} - \lambda(f_1^{EO}(u_1^{j,n}, u_1^{j+1,n}) - f_1^{EO}(u_1^{j-1,n}, u_1^{j,n}))))). \end{aligned}$$

Note here that we have $c(1 - u_2^{j,n}) - (1 - u_1^{j,n}) = v_2^{j,n} - v_1^{j,n}$. We will now use the simplifying notation $\delta v_j^n = v_2(u_2^{j,n}) - v_1(u_1^{j,n})$. Inserting this into the above equation, moving terms around, and using (4.11) we get,

$$\begin{aligned} \frac{\delta v_j^{n+\frac{1}{2}} - \delta v_j^n}{\Delta t} \Delta x &= c(f_2(u_2^{j,n} \wedge \omega) - f_2(u_2^{j,n} \vee \omega) + f_2(u_2^{j+1,n} \vee \omega) - f_2(u_2^{j-1,n} \wedge \omega)) \\ &\quad - (f_1(u_1^{j,n} \wedge \omega) - f_1(u_1^{j,n} \vee \omega) + f_1(u_1^{j+1,n} \vee \omega) - f_1(u_1^{j-1,n} \wedge \omega)) \\ &= c\Gamma_2^j(u_2^n) - \Gamma_1^j(u_2^n) = c^2\Gamma_1^j(u_2^n) - \Gamma_1^j(u_1^n). \end{aligned}$$

Where we define $\Gamma_i^j(u_i^n) := f_i(u_i^{j,n} \wedge \omega) - f_i(u_i^{j,n} \vee \omega) + f_i(u_i^{j+1,n} \vee \omega) - f_i(u_i^{j-1,n} \wedge \omega)$.

We now need to add the additional assumption that $u_{i,0}$ is increasing in both lanes. Recall that Lemma 5.1 guarantees that the solution will then stay increasing in both lanes. Under this assumption we look at the different cases for $\Gamma_i^j(u_i^n)$,

$$\Gamma_i^j(u_i^n) = \begin{cases} f_i(u_i^{j,n}) - f_i(u_i^{j-1,n}), & u_i^{j-1,n} \leq u_i^{j,n} \leq u_i^{j+1,n} \leq \omega \\ f_i(u_i^{j+1,n}) + f_i(u_i^{j,n}) - f_i(\omega) - f_i(u_i^{j-1,n}), & u_i^{j-1,n} \leq u_i^{j,n} \leq \omega \leq u_i^{j+1,n} \\ f_i(u_i^{j+1,n}) + f_i(\omega) - f_i(u_i^{j,n}) - f_i(u_i^{j-1,n}), & u_i^{j-1,n} \leq \omega \leq u_i^{j,n} \leq u_i^{j+1,n} \\ f_i(u_i^{j+1,n}) - f_i(u_i^{j,n}), & \omega \leq u_i^{j-1,n} \leq u_i^{j,n} \leq u_i^{j+1,n}. \end{cases}$$

Thus it follows that

$$\sum_{j \in \mathbb{Z}} \Gamma_i^j(u_i^n) = f_i(u_{i,r}) - f_i(u_{i,l}).$$

Finally, we use this to conclude that

$$\sum_{j \in \mathbb{Z}} \frac{\delta v_j^{n+\frac{1}{2}} - \delta v_j^n}{\Delta t} \Delta x = c(f_2(u_{2,r}) - f_2(u_{2,l})) - (f_1(u_{1,r}) - f_1(u_{1,l})). \quad (5.11)$$

We can see that this seems quite related to the value of \mathcal{G}_n though missing some absolute values. However, we can circumvent this problem by noting the following

$$\begin{aligned} \Gamma_i^j(u_i^n) &\geq 0, \quad \text{for } u_i^{j-1,n} \leq u_i^{j,n} \leq u_i^{j+1,n} \leq \omega \\ \Gamma_i^j(u_i^n) &\leq 0, \quad \text{for } \omega \leq u_i^{j-1,n} \leq u_i^{j,n} \leq u_i^{j+1,n}. \end{aligned}$$

Thus if we require initial conditions satisfying

$$u_1^{j,0} \leq u_1^{j+1,0} \leq \omega \leq u_2^{j,0} \leq u_2^{j+1,0}, \quad (5.12)$$

for every $j \in \mathbb{Z}$, we get that $\delta v_j^n > 0$. This allows us to conclude that asymptotically we will have $v_1(u_1^{j,n}) \geq v_2(u_2^{j,n})$. Thus we will for the remaining analysis assume this to be the case. With this established we can then conclude that

$$\mathcal{G}_n = \sum_{j \in \mathbb{Z}} \frac{\delta v_j^{n+\frac{1}{2}} - \delta v_j^n}{\Delta t} \Delta x = c(f_2(u_{2,r}) - f_2(u_{2,l})) - (f_1(u_{1,r}) - f_1(u_{1,l})) > 0.$$

Next we look at the source step. We suppose now that (4.22) is satisfied. Then we get that

$$\begin{aligned}
|\delta v_j^{n+1}| - \left| \delta v_j^{n+\frac{1}{2}} \right| &= \delta v_j^{n+1} - \delta v_j^{n+\frac{1}{2}} \\
&= \left(c(u_2^{j,n+\frac{1}{2}} - u_2^{j,n+1}) - (u_1^{j,n+\frac{1}{2}} - u_1^{j,n+1}) \right) \\
&= \Delta t S(u_1^{j,n+\frac{1}{2}}, u_2^{j,n+\frac{1}{2}})(c+1) \\
&= \Delta t (c+1) \delta v_j^{n+\frac{1}{2}} u_2^{j,n+\frac{1}{2}}
\end{aligned}$$

Since we know this to be negative, and since $u_2^l \leq u_2^{j,n+\frac{1}{2}} \leq u_2^r$, we then get the bounds

$$u_2^l (c+1) \delta v_j^{n+\frac{1}{2}} \geq \frac{\left(|\delta v_j^{n+1}| - \left| \delta v_j^{n+\frac{1}{2}} \right| \right)}{\Delta t} \geq u_2^r (c+1) \delta v_j^{n+\frac{1}{2}}. \quad (5.13)$$

We can then multiply by $-\Delta x$, and sum over j to get

$$u_2^l (c+1) \mathcal{F}(u^{n+\frac{1}{2}}) \leq -\mathcal{H}_n \leq u_2^r (c+1) \mathcal{F}(u^{n+\frac{1}{2}}). \quad (5.14)$$

Finally, asymptotically we will have $\mathcal{H}_n = \mathcal{G}_n$, which finally gives us an asymptotic bound on $\mathcal{F}(u^n)$. Since we have not proven that $\mathcal{F}(u^n)$ converges, we make this more precise statement. Given $\varepsilon > 0$, there exists N such that for every $n \leq N$, we have

$$\frac{c(f_2(u_{2,r}) - f_2(u_{2,l})) - (f_1(u_{1,r}) - f_1(u_{1,l}))}{(c+1)u_2^r} - \varepsilon \leq \mathcal{F}(u^n) \quad (5.15)$$

$$\frac{c(f_2(u_{2,r}) - f_2(u_{2,l})) - (f_1(u_{1,r}) - f_1(u_{1,l}))}{(c+1)u_2^l} + \varepsilon \geq \mathcal{F}(u^n). \quad (5.16)$$

We see here that this shows that \mathcal{F} does not go to zero asymptotically. We note also that this fits in well with the numerical results we have obtained thus far. In particular, the results in Figure 6 fit exactly within the above bounds.

We give a final remark that it would not be difficult to do a similar construction using only decreasing initial conditions instead.

6 Conclusion and further work

Through a combination of numerical simulations and analytical methods, we have investigated the long-term behaviour of traffic flow on long roads with two lanes of unidirectional traffic. Specifically, we have studied in-depth how the difference in velocity between the two lanes has develops in the long term. One of these findings is that, $\mathcal{F}(u(\cdot, t))$ does not generally go to zero asymptotically. We found this primarily through counterexamples, where $\mathcal{F}(u(\cdot, t))$ did not go to zero. However, in all examples that we have examined the $\mathcal{F}(u(\cdot, t))$ did seem to converge to some value asymptotically.

Based on these results, it seems natural to suppose the asymptotic behaviour will depend mainly on how great of an increase/ decrease we see across the entire length of road, i.e.

$$\lim_{x \rightarrow \infty} u_{1/2,0}(x) - \lim_{x \rightarrow -\infty} u_{1/2,0}(x).$$

A more exact proof of this conjecture, preferably with some bound similar to (5.15), would be interesting for further work. Though such a project might not actually be very useful.

Further work would also include doing a similar analysis for the case where we have d lanes of unidirectional traffic. We believe this expansion to multiple lanes of the current study should not be very complicated. However, it has not been prioritized for this thesis.

It would also be interesting to see what behaviour appears in situations where we look at solutions not on the real line, but on some bounded interval. In this case there are many interesting boundary conditions which could be imposed. In particular, we note that when we were using the periodic boundary conditions for our simulations, the total variation seems to always go to zero.

A Scaling the traffic equation

Here we provide a short rundown of how we might rescale the traffic equation. We start out with the density of vehicles in lane i , $u_i^*(x^*, t^*)$ with unit $[u_i^*] = \frac{\text{vehicles}}{m}$. Furthermore, u_{\max} denotes the maximal density of vehicles, which we assume to be the same in both lanes.

Then we assume the velocity of vehicles to be decided only by the density of traffic. We then suppose $v_i^*(u_i^*)$ to be the velocity function in lane i , with unit $[v_i^*] = \frac{m}{s}$. We assume then that $v_i^*(u_{\max}) = 0$, $v_i^*(0) = v_{i,\max}$, that v_i^* is differentiable, and strictly decreasing. The unscaled traffic equation is then given by

$$\partial_{t^*} u_i^* + \partial_{x^*} (u_i^* v_i^*(u_i^*)) = (-1)^i K (v_2^*(u_2^*) - v_1^*(u_1^*)) \begin{cases} u_2^*, & v_2^*(u_2^*) \leq v_1^*(u_1^*), \\ u_1^*, & v_2^*(u_2^*) > v_1^*(u_1^*), \end{cases} \quad (\text{A.1})$$

where K is some positive constant with unit $[K] = \frac{1}{m}$. This gives the unit $\frac{\text{vehicles}}{ms}$ on both sides of the equality.

We start out scaling by using characteristic scales $x^* = Lx$, and $t^* = Tt$. Which gives units $[T] = s$, $[L] = m$, and $[t] = [x] = 1$. Then define

$$u_i(x, t) = \frac{u_i^*(Lx, Tt)}{u_{\max}}, \quad \tilde{v}_i(u_i) = v_i^*(u_i u_{\max}). \quad (\text{A.2})$$

This gives us the equalities

$$\partial_t u_i = \frac{T}{u_{\max}} \partial_{t^*} u_i^*, \quad \partial_x (u_i \tilde{v}_i(u_i)) = \frac{L}{u_{\max}} \partial_{x^*} (u_i^* v_i^*) \quad (\text{A.3})$$

Where the last equality is obtained by noting first that $\tilde{v}_i'(u_i) = u_{\max} (v_i^*)'(u_i^*)$, which in turn directly implies $u_i \tilde{v}_i' = u_i^* v_i^*$. This allows us to do the derivation

$$\begin{aligned} \partial_x (u_i \tilde{v}_i(u_i)) &= (\partial_x u_i) (\tilde{v}_i(u_i) + u_i \tilde{v}_i'(u_i)) \\ &= \frac{L}{u_{\max}} (\partial_{x^*} u_i^*) (v_i^*(u_i^*) + u_i^* v_i^*(u_i^*)) \\ &= \frac{L}{u_{\max}} \partial_{x^*} (u_i^* v_i^*(u_i^*)). \end{aligned}$$

Finally, this lands us on the equation

$$\frac{u_{\max}}{T} \partial_t u_i + \frac{u_{\max}}{L} \partial_x (u_i \tilde{v}_i(u_i)) = (-1)^i K (\tilde{v}_2(u_2) - \tilde{v}_1(u_1)) \begin{cases} u_{\max} u_2, & v_2(u_2) \leq v_1(u_1), \\ u_{\max} u_1, & v_2(u_2) > v_1(u_1). \end{cases} \quad (\text{A.4})$$

We see that we can divide away u_{\max} . Furthermore, we multiply by T to obtain the expression

$$\partial_t u_i + \frac{T}{L} \partial_x (u_i \tilde{v}_i(u_i)) = (-1)^i K T (\tilde{v}_2(u_2) - \tilde{v}_1(u_1)) \begin{cases} u_2, & v_2(u_2) \leq v_1(u_1) \\ u_1, & v_2(u_2) > v_1(u_1). \end{cases} \quad (\text{A.5})$$

Finally, we choose $T = \frac{1}{K v_{1,\max}}$, and $L = T v_{1,\max}$. We define then $v_i(u_i) = \frac{\tilde{v}_i(u_i)}{v_{1,\max}}$, which at last gives us the rescaled, dimensionless traffic equation

$$\partial_t u_i + \partial_x (u_i v_i(u_i)) = (-1)^i (v_2(u_2) - v_1(u_1)) \begin{cases} u_2, & v_2(u_2) \leq v_1(u_1), \\ u_1, & v_2(u_2) > v_1(u_1), \end{cases} \quad (\text{A.6})$$

where we have that $v_1(0) = 1$, and $v_2(0) = c = \frac{v_{2,\max}}{v_{1,\max}}$.

We end this appendix by making the remark the velocity function need not be bounded at density zero. For instance, the Greenberg model [7] is unbounded as $u \rightarrow 0$. In such a case, we would do a similar procedure when scaling the equation, replacing $v_{i,\max}$ by some characteristic velocity instead.

References

- [1] B. Argall, C. Hinde, E. Cheleshkin, J. M. Greenberg, and P.-J. Lin. A rigorous treatment of a follow-the-leader traffic model with traffic lights present. *SIAM Journal on Applied Mathematics*, 63(1):149–168, 2002.
- [2] O.A. Cirpka, E.O. Frind, and R. Helmig. Numerical simulation of biodegradation controlled by transverse mixing. *Journal of Contaminant Hydrology*, 40(2):159–182, 1999.
- [3] C. Dafermos. *Hyperbolic Conservation Laws in Continuum Physics*, volume 325. Springer New York, 2009.
- [4] B. Engquist and S. Osher. One-sided difference approximations for nonlinear conservation laws. *Mathematics of Computation*, 36(154):321–351, 1981.
- [5] B. Engquist and S. Osher. Upwind difference schemes for systems of conservation laws-potential flow equations. Technical report, Winsconsin univ-Madison mathematics research center, 1981.
- [6] D.C. Gazis, R. Herman, and R.W. Rothery. Nonlinear follow-the-leader models of traffic flow. *Operations Research*, 9(4):545–567, 1961.
- [7] H. Greenberg. An analysis of traffic flow. *Operations Research*, 7(1):79–85, 1959.
- [8] B.D. Greenshields, J.R. Bibbins, W.S. Channing, and H.H. Miller. A study of traffic capacity. *Highway Research Board proceedings*, 14(1):448–477, 1935.
- [9] H. Hanche-Olsen, H. Holden, and E. Malinnikova. An improvement of the kolmogorov-riesz compactness theorem. *Expositiones Mathematicae*, 37(1):84–91, 2019.
- [10] H. Holden. *Tools from the Toolbox - Functional Analysis for Partial Differential Equations*. Unpublished, 2021.
- [11] H. Holden, K. Karlsen, K.-A. Lie, and N. H. Risebro. *Splitting methods for partial differential equations with rough solutions. Analysis and Matlab programs*. European Mathematical Society, 2010.
- [12] H. Holden, K. Karlsen, and N. H. Risebro. On uniqueness and existence of entropy solutions of weakly coupled systems of nonlinear degenerate parabolic equations. *Electronic Journal of Differential Equations*, 2003(46):1–31, 2003.
- [13] H. Holden and N. H. Risebro. The continuum limit of follow-the-leader models - a short proof. *Discrete and Continuous Dynamical Systems*, 38(2):715–722, 2018.
- [14] H. Holden and N. H. Risebro. Follow-the-leader models can be viewed as a numerical approximation to the lighthill-whitham-richards model for traffic flow. *Networks & Heterogeneous Media*, 13:409–421, 2018.
- [15] H. Holden and N. H. Risebro. Models for dense multilane vehicular traffic. *SIAM Journal on Mathematical Analysis*, 51(5):3694–3713, 2019.
- [16] H. Holden and N.H. Risebro. *Front Tracking for Hyperbolic Conservation Laws*. Springer New York, 2015.

- [17] M. J. Lighthill and G. B. Whitham. On kinematic waves. ii. a theory of traffic flow on long crowded roads. *Proceedings of the Royal Society of London. Series A, Mathematical and Physical Sciences*, 229(1178):317–345, 1955.
- [18] R. Natalini and B. Hanouzet. Weakly coupled systems of quasilinear hyperbolic equations. *Differential Integral Equations*, 9(6):1279–1292, 1996.
- [19] Y. Qin. *Integral and Discrete Inequalities and Their Applications*. Birkhäuser Cham, 2016.
- [20] P.I. Richards. Shock waves on the highway. *Operations Research*, 4(1):42–51, 1956.
- [21] D. Schaeffer and J. Cain. *Ordinary Differential Equations: Basics and Beyond*, volume 65. Springer New York, NY, 2016.
- [22] D. K. Steinsland. Long term behavior of dense vehicular traffic with two lanes. Report for the course TMA4500 - Industrial Mathematics, Specialisation Project, NTNU, 2022. Available online at <https://github.com/danielKSt/tma4500-Danielkst>.
- [23] A. Tordeux, G. Costeseque, M. Herty, and A. Seyfried. From traffic and pedestrian follow-the-leader models with reaction time to first order convection-diffusion flow models. *SIAM Journal on Applied Mathematics*, 78(1):63–79, 2018.

